



Australian Government
Department of Defence
Defence Science and
Technology Organisation

Development and Use of a Dynamic-Testing Capability for the DSTO Water Tunnel

Lincoln P. Erm

Air Vehicles Division
Defence Science and Technology Organisation

DSTO-TR-1836

ABSTRACT

This report gives details of the development and use of a water-tunnel dynamic-testing system, whereby models of aircraft are tested as they undergo a dynamic manoeuvre, with the roll, pitch and yaw angles changing in a specified way. Traditionally, most testing of aircraft in tunnels has been done with the aircraft stationary and set at a known orientation, but the acquired static data has limited applicability to manoeuvring aircraft. Dynamic data are needed to study unsteady aerodynamic effects associated with aircraft motion, to obtain data for use in flight-dynamic models of aircraft behaviour, and when validating CFD predictions of aircraft behaviour. Using the new testing system, flow-induced loads on an aircraft model can be measured and corresponding images of the flow over the aircraft can be captured for known instantaneous orientations of the aircraft, so that the loads can be correlated with the flow patterns. During a dynamic manoeuvre, including a coning manoeuvre, loads and images can also be acquired while simulating engine-intake flows. Loads were measured on a delta wing in the water tunnel when the wing was stationary and when it was in motion. The measured loads showed good agreement with wind- and water-tunnel data reported in the literature, showing that the new testing system gives credible results.

RELEASE LIMITATION

Approved for public release

Published by

*Defence Science and Technology Organisation
506 Lorimer St
Fishermans Bend, Victoria 3207 Australia*

*Telephone: (03) 9626 7000
Fax: (03) 9626 7999*

*© Commonwealth of Australia 2006
AR-013-599
March 2006*

APPROVED FOR PUBLIC RELEASE

Development and Use of a Dynamic-Testing Capability for the DSTO Water Tunnel

Executive Summary

Modern combat aircraft have flight envelopes that encompass rapid manoeuvres at high angles of attack, where the flow is unsteady and highly non-linear. It is essential to have a sound knowledge of the aerodynamics of the flow to help solve any flight-mechanics problems that may occur. Data taken in tunnels can be used to help understand and interpret the physics of the complex flow, and the data should be taken while an aircraft model is in motion, similar to a flight manoeuvre. Most testing of aircraft models in tunnels has been done with the model stationary, but static data have limited applicability when studying the behaviour of manoeuvring aircraft. Dynamic data taken in tunnels are needed for the data bases in flight-dynamic models used to predict aircraft behaviour, and when validating CFD predictions of aircraft behaviour. Such data can be used to supplement data from flight trials using actual aircraft.

In the past, most dynamic testing has been carried out in wind tunnels, rather than water tunnels, but due to similarity requirements, the model motion in a water tunnel can be about 100 times slower than in a wind tunnel, which is a distinct advantage. This consideration, coupled with technological advances in strain-gauge balances, used to measure the very small flow-induced loads on water-tunnel models, means that water-tunnel dynamic-testing systems are now becoming feasible.

This report gives details of the development and use of a water-tunnel dynamic-testing system. For known instantaneous orientations of an aircraft model, forces and moments can be measured and corresponding images of the flow can be captured, so that loads can be correlated with flow patterns. The DSTO system has some significant unique features compared with water-tunnel systems developed elsewhere. In the DSTO facility, it is possible to measure flow-induced loads on an aircraft during a dynamic manoeuvre, including a coning manoeuvre, while simulating engine-intake flow.

Using the new dynamic-testing system, loads were measured on a 70° delta wing when the wing was stationary and when it was in motion. The measurements showed good agreement with wind- and water-tunnel data reported in the literature, showing that data acquired using the new system are credible.

Author



Lincoln P. Erm

Air Vehicles Division

Lincoln Erm obtained a Bachelor of Engineering (Mechanical) degree in 1967 and a Master of Engineering Science degree in 1969, both from the University of Melbourne. His Master's degree was concerned with the yielding of aluminium alloy when subjected to both tensile and torsional loading. He joined the Aeronautical Research Laboratories (now called the Defence Science and Technology Organisation) in 1970 and has worked on a wide range of research projects, including the prediction of the performance of gas-turbine engines under conditions of pulsating flow, parametric studies of ramrocket performance, flow instability in aircraft intakes and problems associated with the landing of a helicopter on the flight deck of a ship. Concurrently with some of the above work, he studied at the University of Melbourne and in 1988 obtained his Doctor of Philosophy degree for work on low-Reynolds-number turbulent boundary layers. Since this time, he has undertaken research investigations in the low-speed wind tunnel and the water tunnel. Recent work has been concerned with developing a technique to measure flow-induced pressures on the surface of a model in the water tunnel and studying jet/vortex interactions in the tunnel.

Contents

NOTATION
1. INTRODUCTION	1
2. EFFECTS OF MOTION ON MEASURED DATA	2
3. WIND TUNNEL VS WATER TUNNEL	3
4. DSTO WATER TUNNEL	4
5. LOAD-MEASUREMENT SYSTEM.....	6
6. NEW MODEL-MOTION SYSTEM	7
6.1 Setup of the Model-Motion System.....	7
6.2 Features of the Roll Mechanism.....	7
6.3 Coning of Model	9
7. OPERATION OF THE DYNAMIC-TESTING SYSTEM	12
7.1 PC and Data-Acquisition Card	12
7.2 Overview of Program WTDR CONTROL	12
7.3 Zeroing Model Orientation Angles	13
7.4 Specification of Required Dynamic Manoeuvre.....	14
7.5 Setting of Pumps/Compressor	15
7.6 Automatic Acquisition of Dynamic Data.....	15
7.6.1 Setting Up and Starting a Manoeuvre	15
7.6.2 Display of Information Throughout a Manoeuvre	15
7.6.3 Writing of Data to Files	18
7.6.4 Dynamic Tare Runs	18
7.6.5 Averaging Loads	18
7.7 Manually Setting Model Roll, Pitch and Yaw Positions	19
7.8 Examination of Dynamic Data	19
7.9 Acquisition of Static Data	21
8. TESTS USING A DELTA WING.....	21
8.1 Details of Delta Wing	21
8.2 Static Pitching Tests	22
8.3 Dynamic Pitching Tests.....	24
8.3.1 Force/Moment Measurements	24
8.3.2 Images of the Flow	27
8.4 Coning Tests.....	27
9. CONCLUDING REMARKS.....	29
10. ACKNOWLEDGEMENTS	30
11. REFERENCES	31

Notation

b	Wingspan of an aircraft, (m).
C_L	Lift force coefficient, (non-dimensional) $C_L = L/(0.5\rho U^2 S)$.
C_m	Pitching-moment coefficient, (non-dimensional), $C_m = m/(0.5\rho U^2 S \bar{c})$.
C_N	Normal-force coefficient, (non-dimensional), $C_N = Z/(0.5\rho U^2 S)$.
C_0	Root chord of delta wing, (m), $C_0 = 0.3$ m.
\bar{c}	Mean aerodynamic chord (mac) of a model, (m).
f	Equivalent constant circular frequency of rotation for pitching motion, (Hz).
k	Reduced frequency of oscillation for pitching motion, (non-dimensional), $k = \pi f \bar{c} / U$.
L	Lift force on an aircraft, (N).
l, m, n	Rolling, pitching and yawing moments respectively associated with the balance and the model coordinate systems, (N.m). Positive directions are given on Figure 15.
S	Plan-view projected area of a model at $\alpha = 0^\circ$, (m ²).
t	Time from the start of a dynamic manoeuvre, (s).
U	Free-stream velocity in the test section of a tunnel, (m/s).
X, Y, Z	Axial, side and normal forces respectively associated with the balance and the model coordinate systems, (N). Positive directions are given on Figure 15.
x, y, z	Axes for the balance and model coordinate systems. Positive directions are given on Figure 15.

Greek Letters

α	Angle of attack, (deg).
α_0	Mean angle of attack, (deg), (used in dynamic tests).
β	Angle of sideslip, (deg).
$\Delta\alpha$	Incremental change in α , (deg), (used in dynamic tests).
ρ	Density of air or water, (kg/m ³).
ϕ, θ, ψ	Roll, pitch and yaw angles respectively, (deg).
$\dot{\phi}, \dot{\theta}, \dot{\psi}$	Roll, pitch and yaw rate respectively of a model, (rad/s).
Φ, Θ, Ψ	Non-dimensional roll, pitch and yaw rate respectively of a model, $\Phi = \dot{\phi} \bar{c} / (2U)$, $\Theta = \dot{\theta} \bar{c} / (2U)$, $\Psi = \dot{\psi} \bar{c} / (2U)$.
Ω	Non-dimensional coning rate of a model about the coning roll axis, $\Omega = \omega b / (2U)$.
ω	Rate of rotation of a model about the coning roll axis shown in Figure 6, (rad/s). Positive direction of rotation is clockwise when looking upstream.

Acronyms

CFD	Computational Fluid Dynamics.
DSTO	Defence Science and Technology Organisation.
UCAV	Unmanned Combat Air Vehicle.

1. Introduction

Forces and moments on aircraft models in wind and water tunnels have generally been measured with the aircraft stationary and set at a known orientation, and likewise for the capture of images of the flow over the aircraft. This static testing is the most common form of testing carried out in tunnels and there is an abundance of useful static measurements reported in the literature. On the other hand, dynamic testing of aircraft models simply means that measurements are taken while the aircraft is in motion, undergoing some manoeuvre. Reported dynamic data are somewhat limited compared with static data, due to practical difficulties of obtaining the dynamic data.

There is a need to carry out dynamic testing on combat aircraft in tunnels to study unsteady aerodynamic effects associated with aircraft motion, as this may have a major impact on the manoeuvrability and controllability of aircraft, especially at high angles of attack. During manoeuvring, the flow over combat aircraft is complex and aircraft can experience attached and totally separated flows, as well as vortical flows with and without bursting –see Suárez *et al.* (1994). A clear understanding of the behaviour of the complex flows is an essential requirement for solving flight-mechanics problems associated with advanced manoeuvring. Dynamic force and moment data are also needed to estimate aerodynamic derivatives used in flight-dynamic models of aircraft behaviour, and when validating CFD predictions of aircraft behaviour. The dynamic load measurements taken in tunnels can be used to supplement data from flight trials on full-size aircraft.

In this report, details are given of the development and use of a dynamic-testing system for the water tunnel at the Defence Science and Technology Organisation (DSTO). The model support system on the tunnel has been upgraded so that it is now possible to impart accurately controlled roll, pitch and yaw motions to a model. Previously it was only possible to impart yaw and pitch motions, but the motions could not be controlled with precision. A mechanism has been built to enable coning experiments to be carried out, whereby an aircraft at an angle of attack is rolled about an axis parallel to the direction of the tunnel free-stream velocity. A sensitive low-load-range two-component strain-gauge balance has been built to measure normal forces and pitching moments on a model in the water tunnel and a five-component balance is currently being manufactured. Details of the two-component balance and ancillary instrumentation are given by Erm (2006). The operation of the dynamic-testing system, including data acquisition and reduction, is controlled via a PC using dedicated software.

For the dynamic-testing system, acquisition of data has been synchronised so that forces and moments on an aircraft and images of the flow over the aircraft are acquired simultaneously throughout a manoeuvre at fixed instants of time corresponding to known aircraft orientations. Instantaneous loads throughout the manoeuvre can therefore be directly correlated with corresponding observed detailed flow patterns at these orientations.

The DSTO dynamic-testing system is a major step forward compared with other systems, such as that developed by Suárez *et al.* (1994). For the DSTO system, a special roll mechanism has been designed so that dye can be discharged from ports on an aircraft and water can be sucked through its intake(s), to simulate engine-intake flows, while the aircraft undergoes continuous roll, i.e. there is no twisting of dye or suction tubes. It is now possible to measure flow-induced loads and capture images of the flow during a dynamic manoeuvre, including a coning manoeuvre, while simulating engine-intake flows.

Normal forces and pitching moments were measured on a delta wing in the DSTO water tunnel when the wing was stationary and when it was in motion. The measurements showed good agreement with corresponding published wind- and water-tunnel data, showing that data acquired using the dynamic-testing system are credible, at least for models with sharp leading edges, where the flow patterns are independent of Reynolds number and are similar to those for full-size vehicles. Comprehensive testing programs using different aircraft will be reported at a later date.

Models for the water tunnel can be made quicker and cheaper than for a wind tunnel, so significant savings of time and money could possibly be made by testing in the water tunnel. Using models manufactured using rapid-prototyping methods, such as stereolithography, aircraft aerodynamic data bases for configuration studies can be built quickly. It may also be possible to use water-tunnel data to develop simple six degree-of-freedom flight-dynamic models for aircraft, such as UCAVs.

2. Effects of Motion on Measured Data

The instantaneous flow pattern over an aircraft as it passes through a given orientation is different from that on the aircraft when it is stationary at that orientation, and likewise for the loading on the aircraft. This is due to the fact that the flow over the aircraft and the associated loading take some time to stabilize when the aircraft is moved to a new orientation, i.e. the flow lags the motion. According to Brandon & Shah (1990), there can be a lag time of up to 50 convective time units (one convective time unit is the time required for a fluid particle to travel across the aircraft) before the flow re-establishes itself to the stationary condition.

Figure 1 shows a plot of lift force coefficients, $C_L = L/(0.5\rho U^2 S)$, for a fighter aircraft, obtained from wind-tunnel tests by Brandon & Shah (1990). Both static and dynamic data are shown. The dynamic data corresponds to the aircraft oscillating in pitch by $\pm 10^\circ$, $\pm 20^\circ$ and $\pm 30^\circ$, about a mean angle of attack, α_0 , of 32° . The reduced frequency of oscillation for the pitching motion, $k = \pi f \bar{c} / U$, has a value of 0.0226, where f is the equivalent constant circular frequency of rotation for the pitching motion and \bar{c} is the mean aerodynamic chord of the aircraft. The measured dynamic C_L vs α data for increasing α is different from that for decreasing α , creating hysteresis loops in the plotted data, so that the instantaneous loading on the aircraft varies over a wide range.

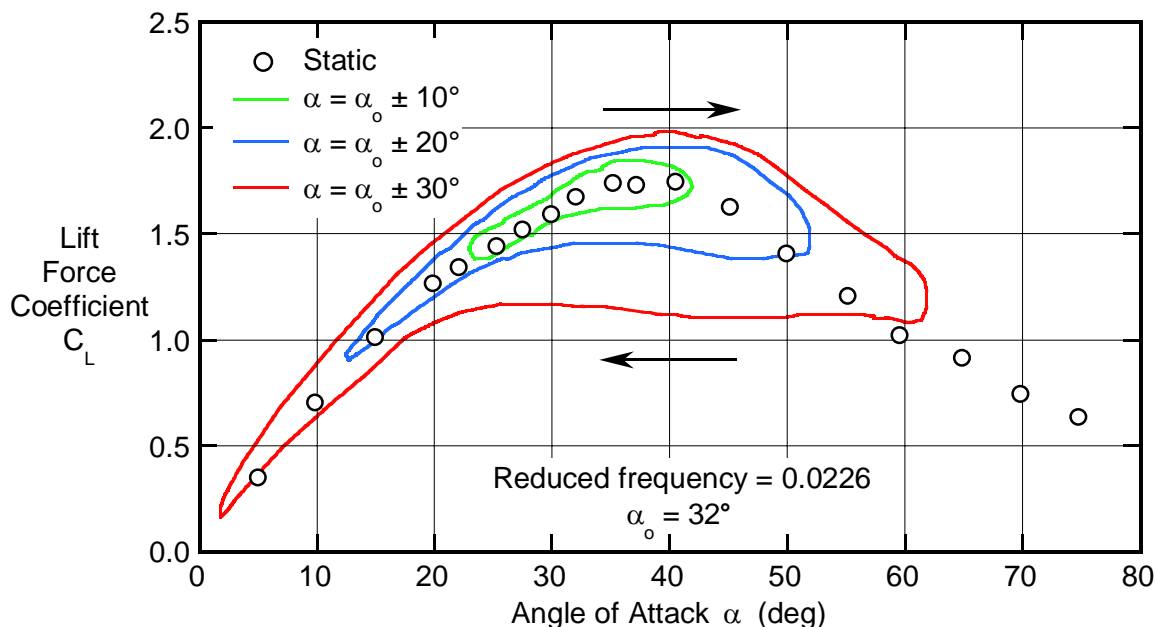


Figure 1. Dynamic wind-tunnel tests using a model of an F-18 aircraft, as obtained by Brandon & Shah (1990).

3. Wind Tunnel vs Water Tunnel

A fundamental principle of dynamic testing is that the non-dimensional pitch rate, $\Theta = \dot{\theta} \bar{c} / (2U)$, of an aircraft model in a tunnel must be the same as that for a full-size aircraft, where $\dot{\theta}$ is the aircraft pitch rate. Parameters for a full-size aircraft, a model in a wind tunnel and a model in a water tunnel are summarised in Table 1. For typical values of pitch rate, characteristic length and free-stream velocity for a full-size aircraft, the value of Θ is 0.0157. For a 1/9 scale model in a wind tunnel operating at 60 m/s, the pitch rate required for this value of Θ is about 220 deg/s, but for a 1/48 scale model in a water tunnel operating at 0.1 m/s, the corresponding pitch rate is only about 2 deg/s.

The required rotation rate in a wind tunnel to simulate a scaled dynamic manoeuvre is over 100 times greater than that for a water tunnel. The fast model rotation rates required for wind-tunnel tests are mechanically difficult to implement ($\dot{\theta} \approx 220$ deg/s) and the effects of model inertia on the measured forces and moments are significant (Suárez & Malcolm 1995). The high model rotation rates also place demanding requirements on a data-acquisition system to acquire data at high sample rates. In contrast, the model rotation rates required in a water tunnel are low ($\dot{\theta} \approx 2$ deg/s), so that the effects of model inertia on the measured loads are negligible (Suárez & Malcolm 1995). The response rates for a data-acquisition system are also less demanding than for a wind tunnel and are more easily managed. However, smaller models and lower free-stream velocities are normally used for dynamic tests in water tunnels than in wind tunnels, so that the loads on the models and the Reynolds numbers are substantially lower than for wind tunnels. Reynolds numbers for the different cases are shown in Table 1.

Table 1. Modelling parameters for a high-performance aircraft.

	Full-size aircraft	Wind-tunnel model (1/9 scale)	Water-tunnel model (1/48 scale)
Non-dimensional pitch rate of aircraft Θ	0.0157	0.0157	0.0157
Free-stream velocity U (m/s)	100	60	0.1
Mean aerodynamic chord of aircraft \bar{c} (m)	4.510	0.501	0.094
Pitch rate of aircraft $\dot{\theta}$ (rad/s) (deg/s)	0.698 40.0	3.770 216.0	0.0335 1.92
Reynolds number (based on \bar{c})	3×10^7	2×10^6	1×10^4

Although most of the reported investigations on dynamic testing have been undertaken in wind tunnels, rather than water tunnels, there are clearly advantages in using a water tunnel. Consequently, the ancillary equipment used with the DSTO water tunnel has been upgraded to enable dynamic testing to be carried out. The system and its components are described in Sections 4 to 7.

4. DSTO Water Tunnel

The DSTO water tunnel was manufactured by Eidetics International Incorporated¹ and is designated Model 1520. The tunnel, shown in Figure 2, holds about 3790 litres of water and has a horizontal-flow test section 380 mm wide, 510 mm deep and 1630 mm long. It is a recirculating closed-circuit tunnel and there is a free water surface in the test section. The side walls and floor of the test section are made from glass to facilitate flow-visualization studies. The tunnel is constructed so that it is possible to look directly upstream into the test section through a glass window at the downstream end of the diffuser. The free-stream velocity in the test section can be varied between 0 and 0.6 m/s. Downstream of the settling chamber there are flow-conditioning elements, consisting of a perforated stainless-steel plate, a honeycomb and two fibreglass screens. The contraction upstream of the test section has an inlet/outlet area ratio of 6:1. This geometry gives a good velocity distribution and turbulence level, and avoids the likelihood of local flow separations. The free-stream velocity in the test section varies by less than $\pm 2\%$ relative to the average value, the mean flow angularity is less than $\pm 1.0^\circ$ in both pitch and yaw angle, and the turbulence intensity is less than 1.0% RMS, (data as given in the Eidetics Water Tunnel Operations Manual).

¹ Now called Rolling Hills Research Corporation, 420 N. Nash St., El Segundo, CA 90245, USA.

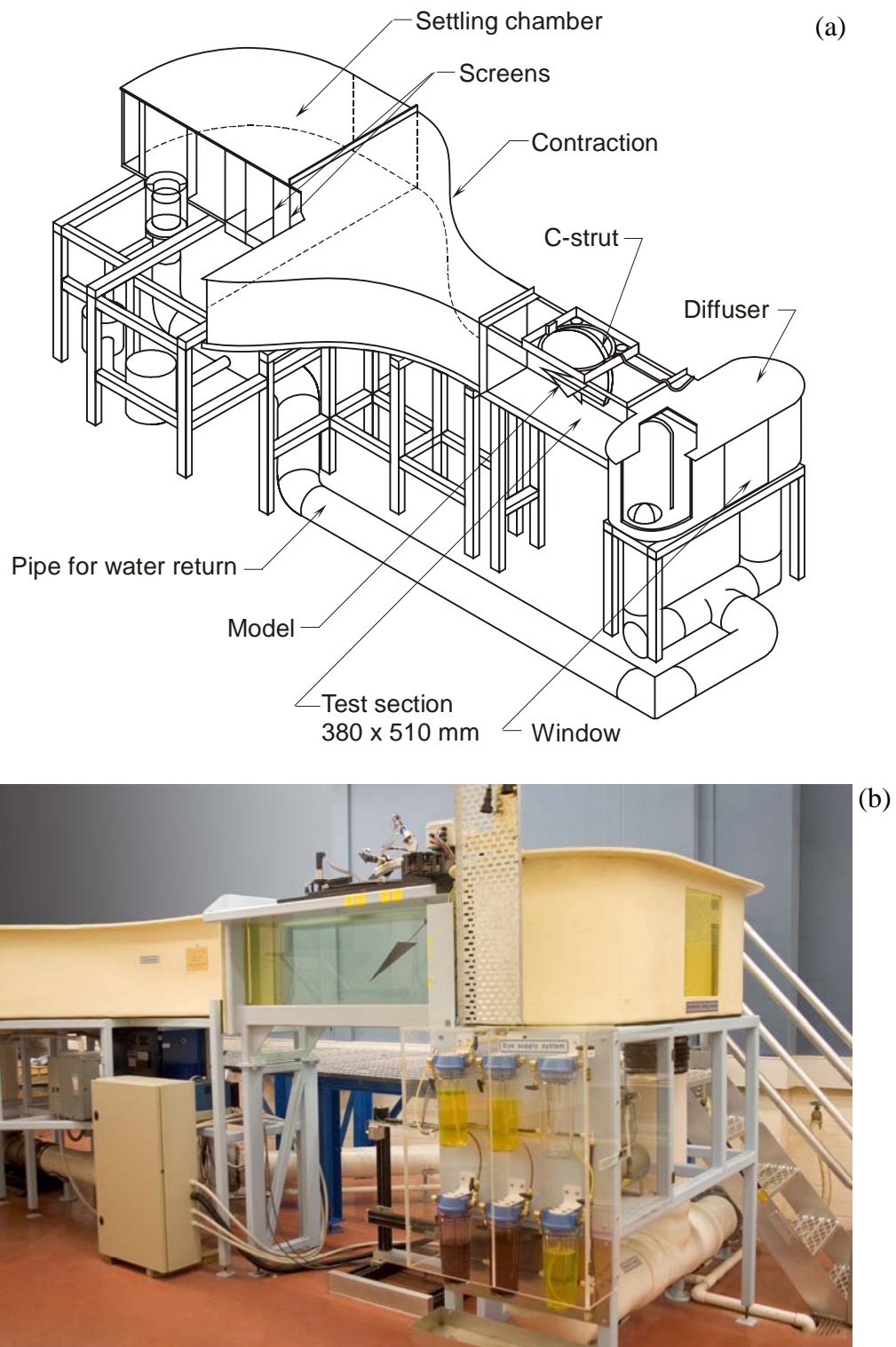


*Figure 2. Eidetics Model 1520 water tunnel.
 (a) diagrammatic view of tunnel, (b) photograph of tunnel.*

There are six dye canisters on the tunnel that can be pressurised with air to force dye through plastic tubes to selected locations on a model for flow-visualization studies. There is a suction pump on the tunnel that can be used to suck or blow water through models. The suction/blower system has two independent circuits, and the maximum volume flow rates through each circuit can be varied between 0 and about 100 ml/s. The flow rates through the dye and suction/blower circuits are controlled by hand-operated valves.

Models are mounted on a C-strut so that the required centre of rotation of a model is at the centre of the imaginary circle formed by the strut, ensuring that all angular motion of the model is about this point. The model supporting system is attached to the top of the test section by a hinge, so that a model can be lowered into the test section, or removed from the test section, as required. When a model has been lowered, its centre of rotation is at the mid transverse position in the test section, 270 mm from the floor and 965 mm downstream of the start of the test section.

5. Load-Measurement System

A load-measurement system has been developed to measure normal forces and pitching moments on a model in the water tunnel. The system is comprised of a sensitive low-load-range two-component strain-gauge balance, a signal-conditioning system and a PC-controlled data-acquisition system. A drawing of the balance, showing the main dimensions, is given in Figure 3. The balance uses sensitive semi-conductor strain gauges and has been designed to measure normal forces and pitching moments within the ranges ± 2.5 N and ± 0.02 N.m respectively. Loads on models are computed using first-order calibration equations. The accuracy of the calibration was checked and the standard errors were found to be 0.1% for the normal-force channel and 0.1% for the pitching-moment channel. A five-component balance is currently being manufactured. Full details of the system for the two-component balance are given by Erm (2006).

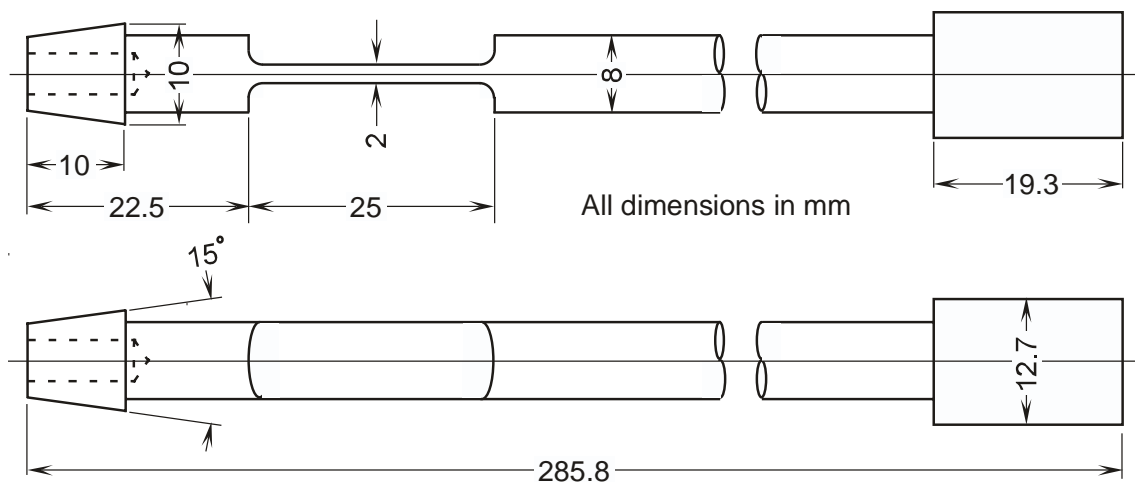


Figure 3. Two-component strain-gauge balance used in the water tunnel.

6. New Model-Motion System

6.1 Setup of the Model-Motion System

Most of the dynamic-testing systems reported in the literature have been limited to model motion in one plane, either roll ϕ , pitch, θ , or yaw, ψ . Huang & Hanff (2001) indicate that since the behaviour of a vortex and its breakdown are non-linear, it is not valid to superimpose the effects due to motion in different planes. There is a need for dynamic testing in which motions in all three planes can be obtained simultaneously. For the original DSTO model-motion system, it was only possible to obtain pitch and yaw motions by manually controlling motors using a joystick, so that motion could not be controlled precisely. Three DC micromotors have now been installed so that precise specified roll, pitch and yaw motions can be controlled independently and simultaneously using a PC. The setup of the upgraded model motion system is shown in Figure 4. Roll, pitch and yaw angles can be varied between 0° and $\pm 360^\circ$, 0° and $+65^\circ$, and -20° and $+20^\circ$ respectively. The required model roll, pitch and yaw angles at chosen instants of time throughout a dynamic manoeuvre are specified by the operator using the PC (see Section 7.4). The range of motions available is virtually unlimited, and includes linear ramped and sinusoidal motions. The maximum obtainable roll, pitch and yaw rotational speeds of a model are 12, 6 and 8 deg/s respectively. It is not possible to impart linear plunging motion to a model, although circular plunging motion can be obtained by mounting a model on a sting that is longer than normal, so that the model no longer rotates about the centre of the imaginary circle formed by the C-strut.

6.2 Features of the Roll Mechanism

A special roll mechanism has been designed so that dye can be discharged from ports on an aircraft model and water can be sucked through its intake(s), while the aircraft undergoes continuous roll, i.e. there is no twisting of dye or suction tubes. The roll mechanism is shown diagrammatically in Figure 4 and cross-sectional views of the mechanism are shown in Figure 5. The chassis of the mechanism is attached to the C-strut and does not rotate. An input shaft from a DC micromotor rotates the central shaft, the strain-gauge balance and the aircraft, via a worm wheel and pinion. A dye reservoir is located between the fixed chassis and a rotating coupling, with the interface sealed with O rings. Dye outlet tubes on the coupling are connected to ports on the aircraft using flexible plastic tubes which rotate with the model. The central shaft on the mechanism is hollow and forms part of the water-flow suction circuit. A suction adaptor is bolted onto the central shaft and the two tubes on the adaptor are connected to circular fittings on the rear of the aircraft using soft flexible silicone tubes. The fittings are connected to the intakes of the aircraft via internal ducting, thereby completing the water-flow circuit. Although the flexible silicone tubes bridge the balance, tests showed that the transmitted loads were very small and could be allowed for by carrying out a tare run (see Section 7.6.4). The hollow central shaft has been partitioned into two halves to enable flows through the two intakes to be controlled independently. The features of the system that enable a model to undergo continuous roll without twisting of dye or suction tubes are believed to be unique.

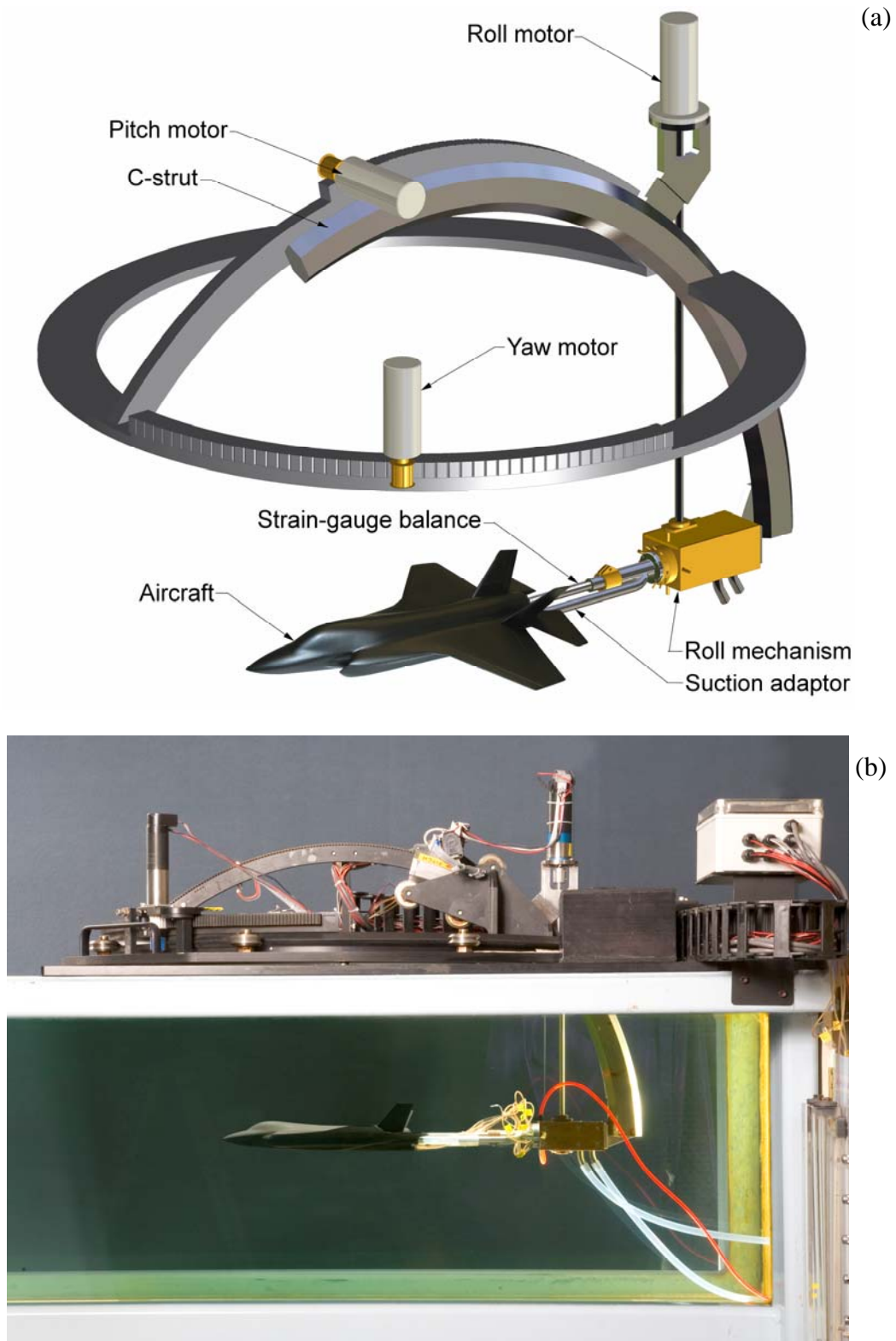


*Figure 4. Upgraded model motion system.
(a) diagrammatic representation of the system, (b) photograph of the system.*

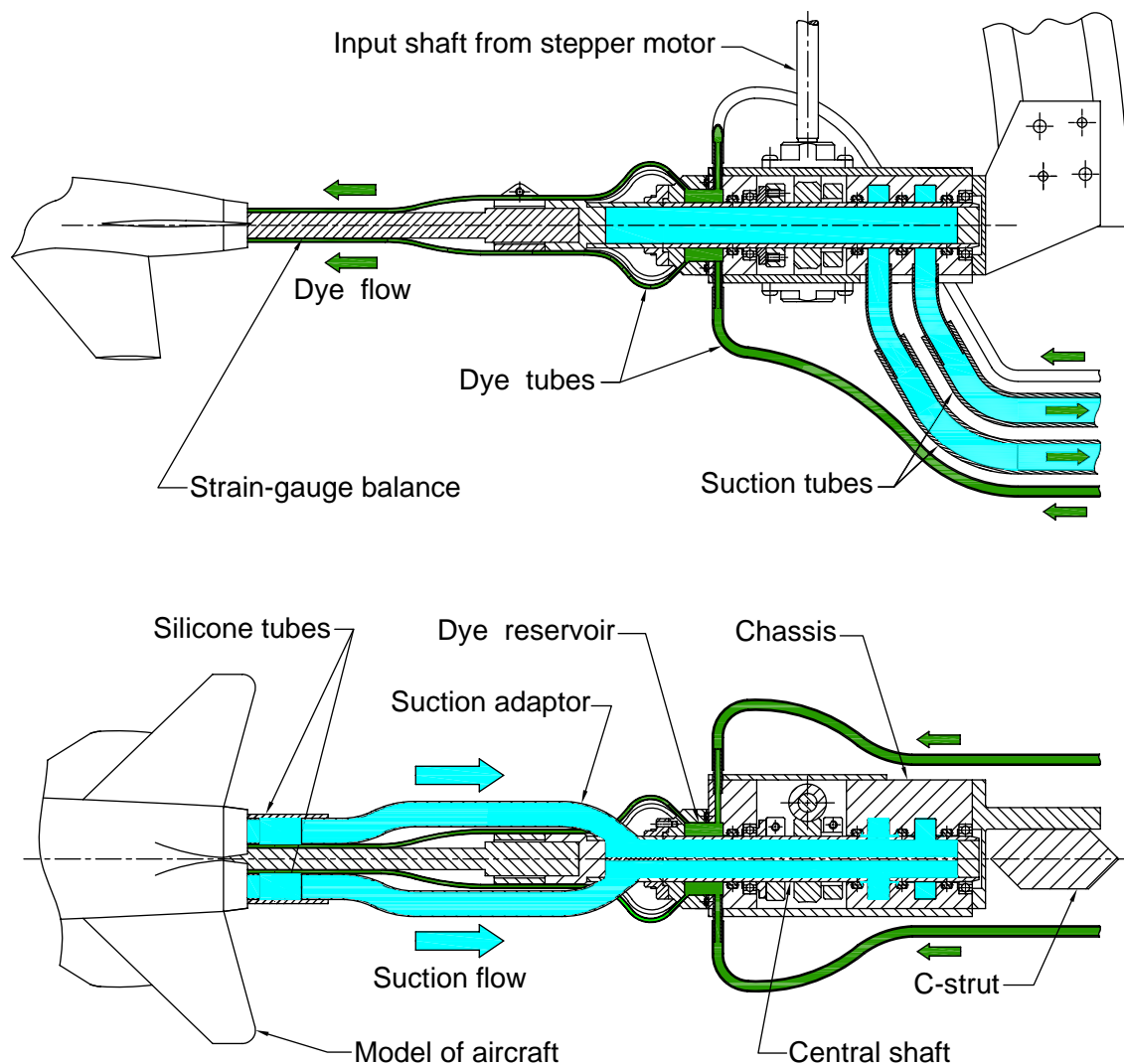


Figure 5. Cross-sectional side- and plan-views of the roll mechanism.

6.3 Coning of Model

Coning or vectored-roll motion occurs when an aircraft, set at a given pitch angle, is rolled at constant angular velocity about an axis that is usually parallel to the free-stream velocity. In the past, coning data was only required for the analysis of the spin and spin-recovery characteristics of aircraft (Orlik-Rückemann & Chambers 1990), but coning motion is now considered to be a key manoeuvre for enhanced agility in combat for fighter aircraft (Kramer *et al.*, 1994). There is a need to carry out coning experiments to help understand the physics of the flow processes involved and to obtain aerodynamic characteristics for use in flight dynamic models.

To generate a coning motion in the water tunnel, an aircraft model is mounted on the coning mechanism, which is attached to the roll mechanism, and rolled about the coning

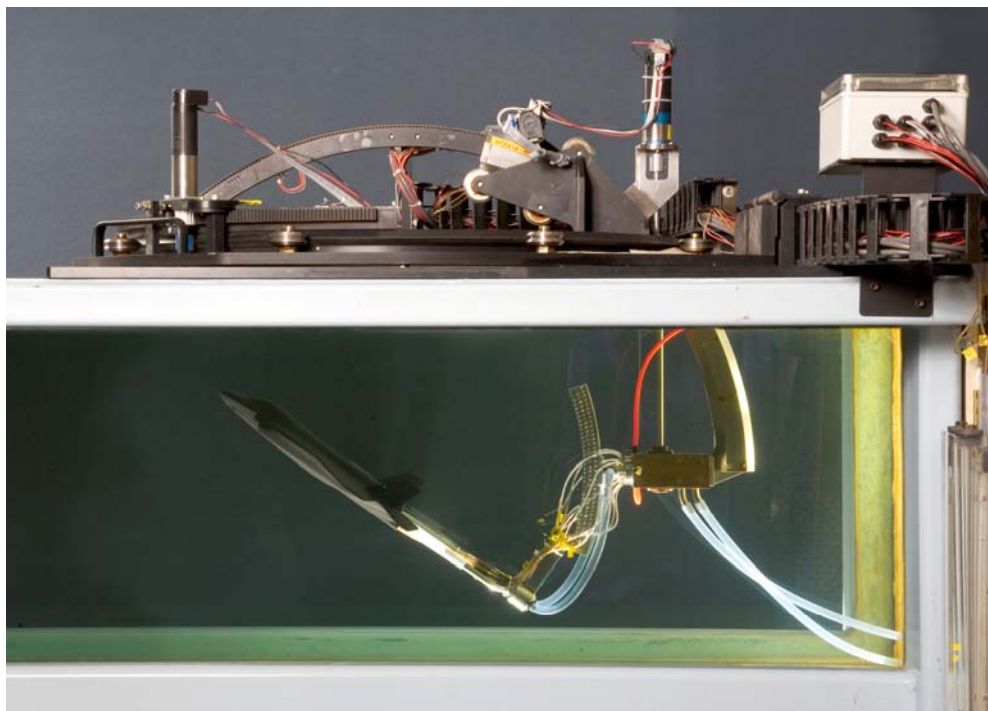
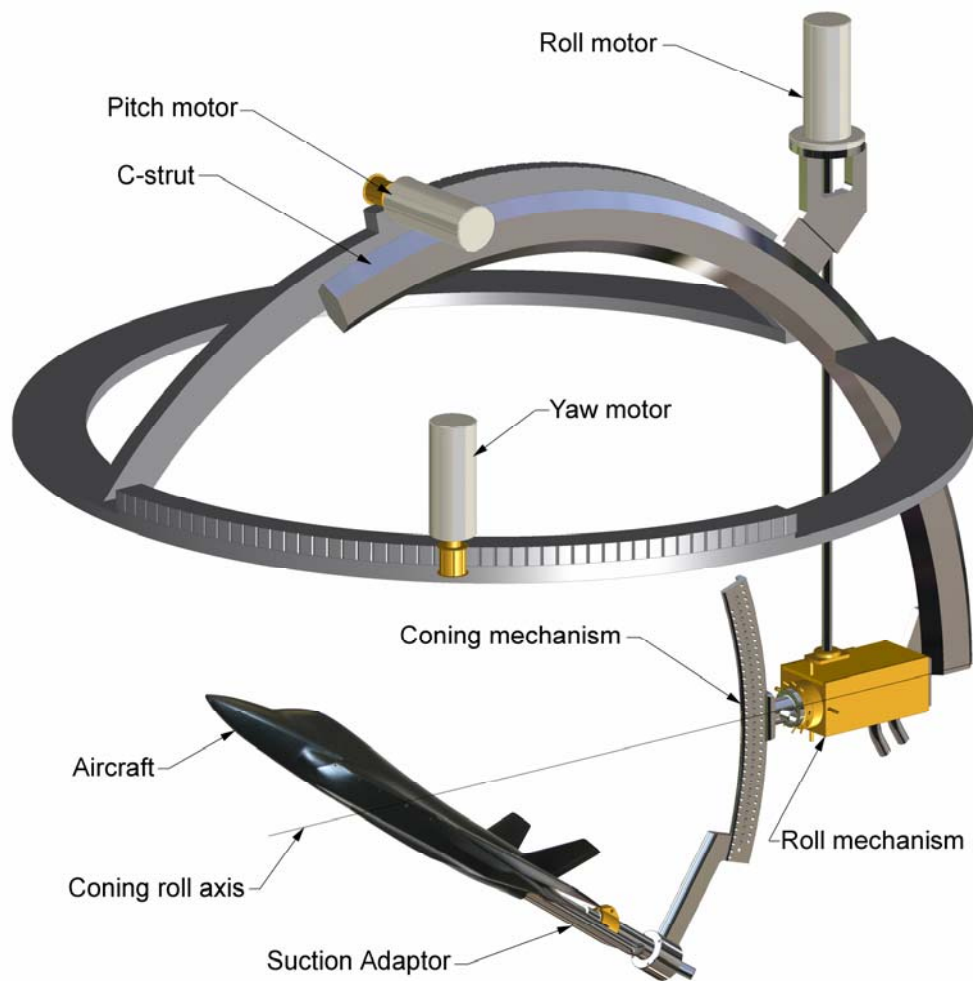
roll axis, as shown in Figure 6. For the coning mechanism shown, the pitch angle can be set between 0° and $+35^\circ$, in 1° increments. The attitude of the model remains constant with respect to the free-stream velocity throughout the coning motion, so that the angles of attack and sideslip, α and β respectively, are also constant throughout the cycle. The pitch angle of 35° is the maximum obtainable in the tunnel using a 1/48 scale model of a typical combat aircraft so that there is acceptable clearance between the mechanism and the side walls of the tunnel during rotation. It is possible to obtain larger coning pitch angles, but it would be necessary to make a new coning mechanism and use a smaller model, such as the 1/72 scale model used by Cai & Beyers (2002) for their coning experiments in a tunnel having test-section cross-sectional dimensions similar to those for the DSTO tunnel. A feature of the DSTO coning setup is that it is possible to measure loads on an aircraft while simulating engine-intake flow during the coning motion.

When carryout out coning experiments in a tunnel, the non-dimensional coning rate, $\Omega = \omega b / (2U)$, of an aircraft model must be the same as that for a full-size aircraft, where ω is the rate of rotation of the aircraft about the coning roll axis (see Figure 6) and b is the wingspan of the aircraft. –see, for example, Ericsson & Beyers (1998). Table 2 summarizes parameters for a typical full-size combat aircraft, a model in a wind tunnel and a model in a water tunnel. For typical values of coning rate, wingspan and free-stream velocity for a full-size aircraft, the value of Ω is 0.150. For a 1/9 scale model in a wind tunnel operating at 60 m/s, the coning rate for this value of Ω is about 870 deg/s (145 rev/min), but for a 1/48 scale model in a water tunnel operating at 0.1 m/s, the coning rate is about 8 deg/s (1.3 rev/min).

Table 2. Coning parameters for a high-performance aircraft.

	Full-sized aircraft	Wind-tunnel model (1/9 scale)	Water-tunnel model (1/48 scale)
Non-dimensional coning rate of aircraft Ω	0.150	0.150	0.150
Free-stream velocity U (m/s)	65.0	60.0	0.1
Wingspan of aircraft b (m)	10.668	1.185	0.222
Coning rate of aircraft ω (rad/s) (deg/s)	1.828 104.7	15.186 870.1	0.1350 7.734

(a)



(b)

Figure 6. Aircraft model mounted on the coning mechanism.
 (a) diagrammatic representation of the mechanism, (b) photograph of the mechanism.

7. Operation of the Dynamic-Testing System

The operation of the water-tunnel dynamic-testing system is controlled using software specially written for the task. Two programs were used, named WTDR CONTROL and WTDR DATA (WT for water tunnel, DR for dynamic rig), that were developed by Motion Solutions² to suit DSTO requirements. The first program was written in Visual Basic 6.0 and the second program was written in Delphi (different languages were used to suit different requirements). WTDR CONTROL is used to set the tunnel free-stream velocity, to control the on/off switches for the dye-flow and the suction-flow pumps, to control the model motion, to sample voltages corresponding to forces and moments on the model, and to control the capture of images of the flow over the model. WTDR DATA is used to examine the synchronised experimental data. The features of WTDR CONTROL are described in Sections 7.2 to 7.7 and those of WTDR DATA in Section 7.8.

7.1 PC and Data-Acquisition Card

The PC used on the dynamic rig has a WindowsTM XP Professional operating system, a 3.2 GHz central processing unit, a 220 GB hard disk drive and 1 GB of RAM.

The data-acquisition card that interfaced with the PC was manufactured by National InstrumentsTM and the product code is NI 6013. The card has 16 channels (8 differential) of 16-bit analog input, a 68 pin connector and 8 lines of digital input/output. Analog input voltages varying between -5 V and +5 V can be sampled. For the 16-bit card, the resolution of the sampled voltages is $10.0/2^{16}$, i.e. $10.0/65536 = 0.000153$ V/LSB = 0.153 mV/LSB (LSB denotes least significant bit).

7.2 Overview of Program WTDR CONTROL

When WTDR CONTROL is launched, the default graphical user interface shown in Figure 7 appears on the monitor. The interface has been designed so that it can be used intuitively when carrying out dynamic tests. On the left-hand side of the interface there are two tabs, named FILE and CONTROL, as well as six icons, named HOME, AUTO, MANUAL, PUMPS, RESULTS and EXIT. The interface also contains six windows, named SCRIPT, CAMERAS, HOMING, ANALOGUE FEEDBACK, POSITION FEEDBACK and STATUS. By clicking on the PUMPS, AUTO and MANUAL icons, the HOMING window is replaced by windows named FLOW/PUMPS, AUTO and MANUAL respectively, as will be shown.

² Motion Solutions Australia Pty Ltd, 21-29 Railway Ave, Huntingdale, Victoria, 3166, Australia.

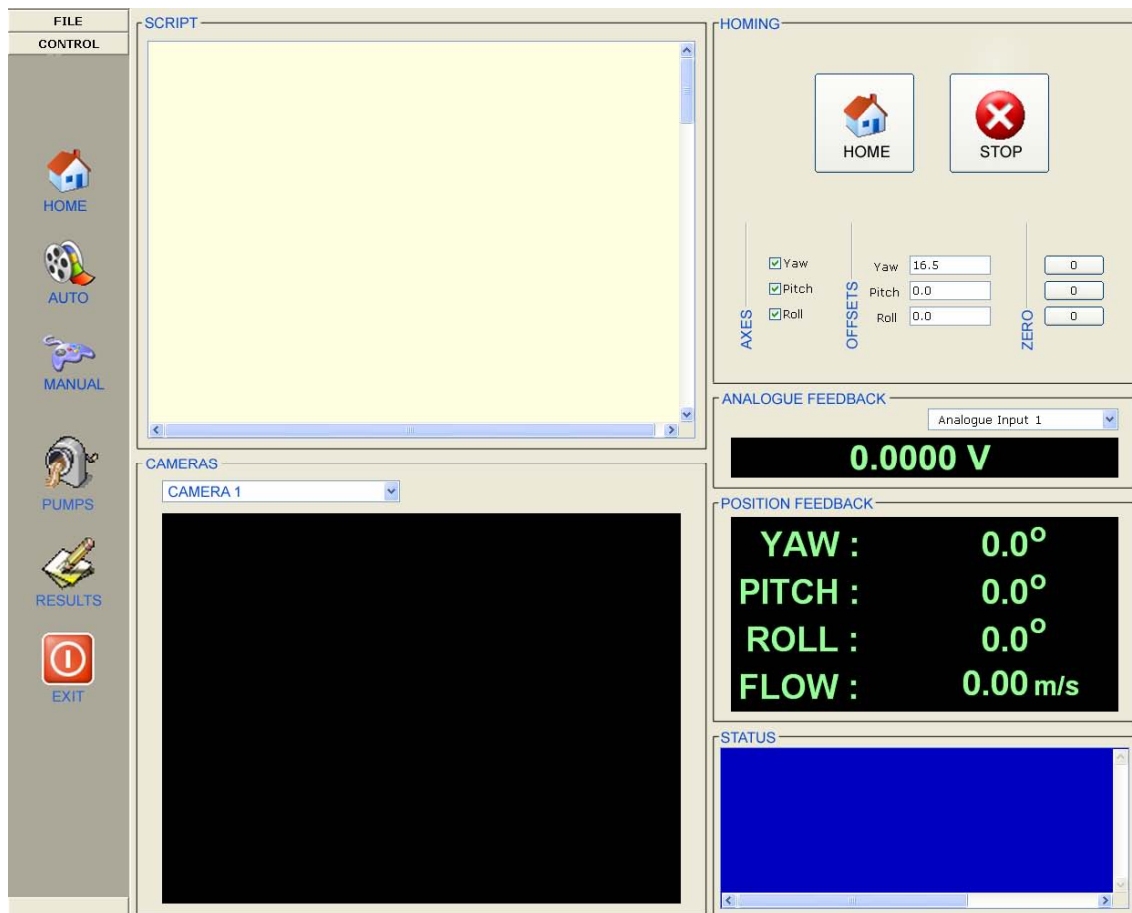


Figure 7. Default graphical user interface.

7.3 Zeroing Model Orientation Angles

When testing, it is crucial that the model orientation is accurately known relative to the coordinates of the test section of the tunnel. When WTDR CONTROL is launched, the exact orientation of the model is generally not known and it is necessary to zero the model roll, pitch and yaw angles before tests can proceed. To set the pitch and yaw angles to 0° , it is necessary to click the HOME button in the HOMING window on the interface, shown in Figure 7. When this is done, the pitch and yaw motors rotate the pitch and yaw mechanisms (see Figure 4) until tabs on the mechanisms reach reference limit switches. The switches are positioned at known offset angles on the rig. When the switches are activated, the direction of rotation of the pitch and yaw motors are reversed and the pitch and yaw angles are then automatically set to 0° . For an aircraft model, the roll angle can be set to 0° using the manual setting procedure (see Section 7.7) until both wing tips of the aircraft simultaneously just touch the surface of the water in the tunnel, with the water not flowing. This setting of the roll angle is then locked in by clicking the ZERO button for the roll axis in the HOMING window on the interface, shown in Figure 7. After the model has been set to its home position, the instantaneous roll, pitch and yaw angles throughout subsequent testing are displayed in the POSITION FEEDBACK window on the interface, shown in Figure 7.

7.4 Specification of Required Dynamic Manoeuvre

Examples of roll, pitch and yaw angles for a dynamic manoeuvre of an aircraft model are shown graphically in Figure 8. This set of orientation angles was chosen somewhat arbitrarily to demonstrate how the system works. The range of dynamic manoeuvres that can be executed by an aircraft model within the orientation envelope is virtually unlimited. Roll, pitch and yaw angles can change linearly or non-linearly with time, and it is possible to oscillate the model in roll, pitch and yaw, with peak angular velocities of 12, 6 and 8 deg/s respectively. Roll, pitch and yaw angles can also be set to be constant throughout all or part of a manoeuvre. It is important to have small dwell periods in the motion whenever large angular velocities in one direction are followed by large angular velocities in the opposite direction, otherwise the motors may be subjected to excessive loading as they attempt to counteract the inertia of the dynamic rig. A limitation of the rig is that it is not possible to impart plunging motion to an aircraft.

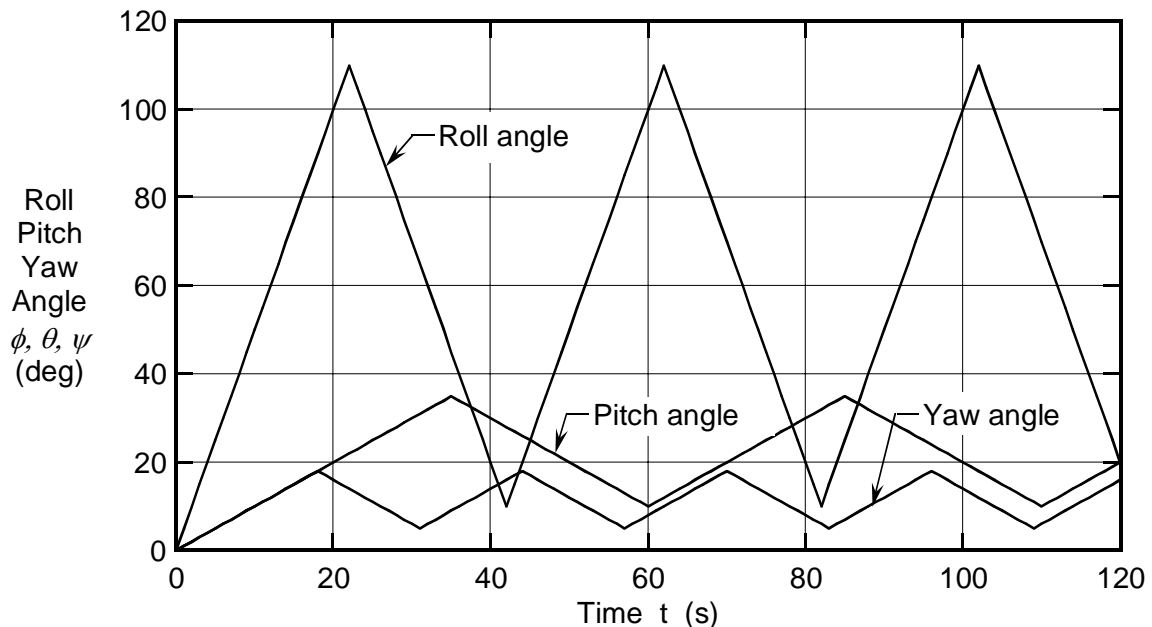


Figure 8. Examples of roll, pitch and yaw angles for a dynamic manoeuvre.

To enable the aircraft to execute the manoeuvre, it is first necessary to create a script file, using Microsoft® Notepad, which contains the required roll, pitch and yaw angles for given instants of time. The script file can be displayed in the SCRIPT window on the interface, as shown in Figure 9, after first clicking on the FILE tab on the left-hand side of the interface and opening the file as instructed. In the script file, T corresponds to time (s), and L, M and N correspond to roll, pitch and yaw angles (deg) respectively. Normally ϕ , θ and ψ are used to denote roll, pitch and yaw angles respectively, but L, M and N were used in this case for programming convenience.

7.5 Setting of Pumps/Compressor

To activate the tunnel water-flow pump, the suction/blower pump or the dye-flow air compressor, it is first necessary to click on the PUMPS icon on the interface so that the FLOW/PUMPS window is displayed, as shown in Figure 10. The dye circuit is pressurised to ensure a “clean” flow of dye through the tubes to the model. The pumps and the compressor can be turned on or off by simply clicking on the appropriate ON or OFF buttons. The free-stream velocity in the test section can be set by dragging the slider along the graduated scale to the required velocity. The free-stream velocity can be set between 0.00 and 0.60 m/s, in increments of 0.01 m/s, i.e. 60 steps. The rates of flow of dye through the dye circuit and water through the engine suction/blower circuit are controlled by hand-operated valves on the tunnel.

7.6 Automatic Acquisition of Dynamic Data

7.6.1 Setting Up and Starting a Manoeuvre

To acquire dynamic data, it is necessary to click the AUTO icon on the interface so that the AUTO window appears, as shown in Figure 11. Before commencing the dynamic manoeuvre, the model has to be reoriented to its home position by clicking the RESET button. After the model has been homed, it is necessary to click the LOAD button to load the script file (appearing in the SCRIPT window) corresponding to the motion required. The RECORD box also has to be checked to indicate that data is to be acquired during the manoeuvre. Finally, it is necessary to click the PLAY button to start the manoeuvre. The STATUS window is used to monitor the different steps throughout a test, and displays information such as “Homing Yaw Axis”, “Homing Pitch Axis”, “Homing Roll Axis”, “Moving to System Offsets”, “System Homed”, and “Script Loaded”.

7.6.2 Display of Information Throughout a Manoeuvre

The progress of the manoeuvre, in terms of the percentage completed, is indicated by a moving bar in the AUTO window, as shown in Figure 12. Instantaneous roll, pitch and yaw angles throughout the manoeuvre are displayed in the POSITION FEEDBACK window as shown. Corresponding output voltages from the signal-conditioning system can also be displayed in the ANALOGUE FEEDBACK window as shown, depending on which channel is selected using the pull-down menu on the window. The CAMERAS window can display corresponding images of the flow over a model, as captured by two SonyTM digital video cameras, model number DCR-VX2100E. Either plan-view or side-view images can be displayed, depending on which camera is selected using the pull-down menu on the window.

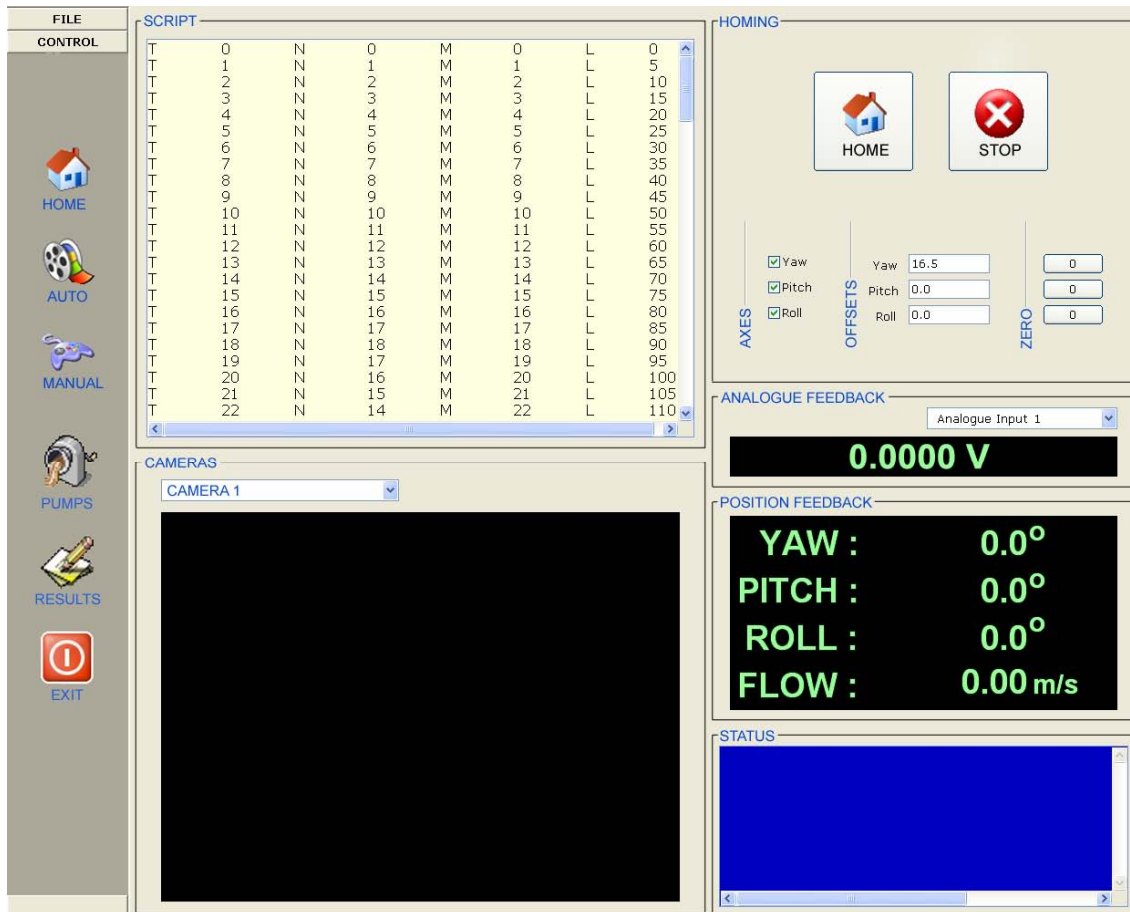


Figure 9. Graphical user interface, showing a script file in the SCRIPT window.

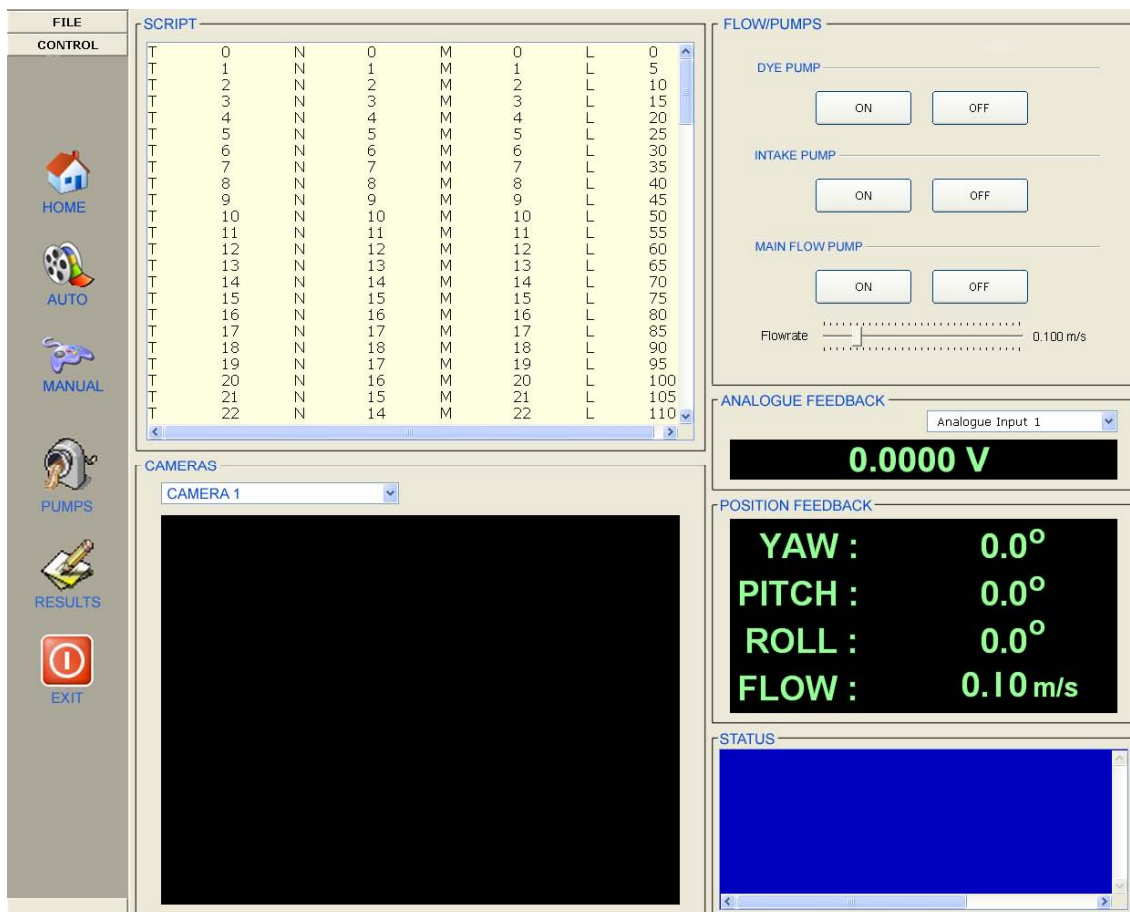


Figure 10. Graphical user interface, showing the FLOW/PUMPS window.

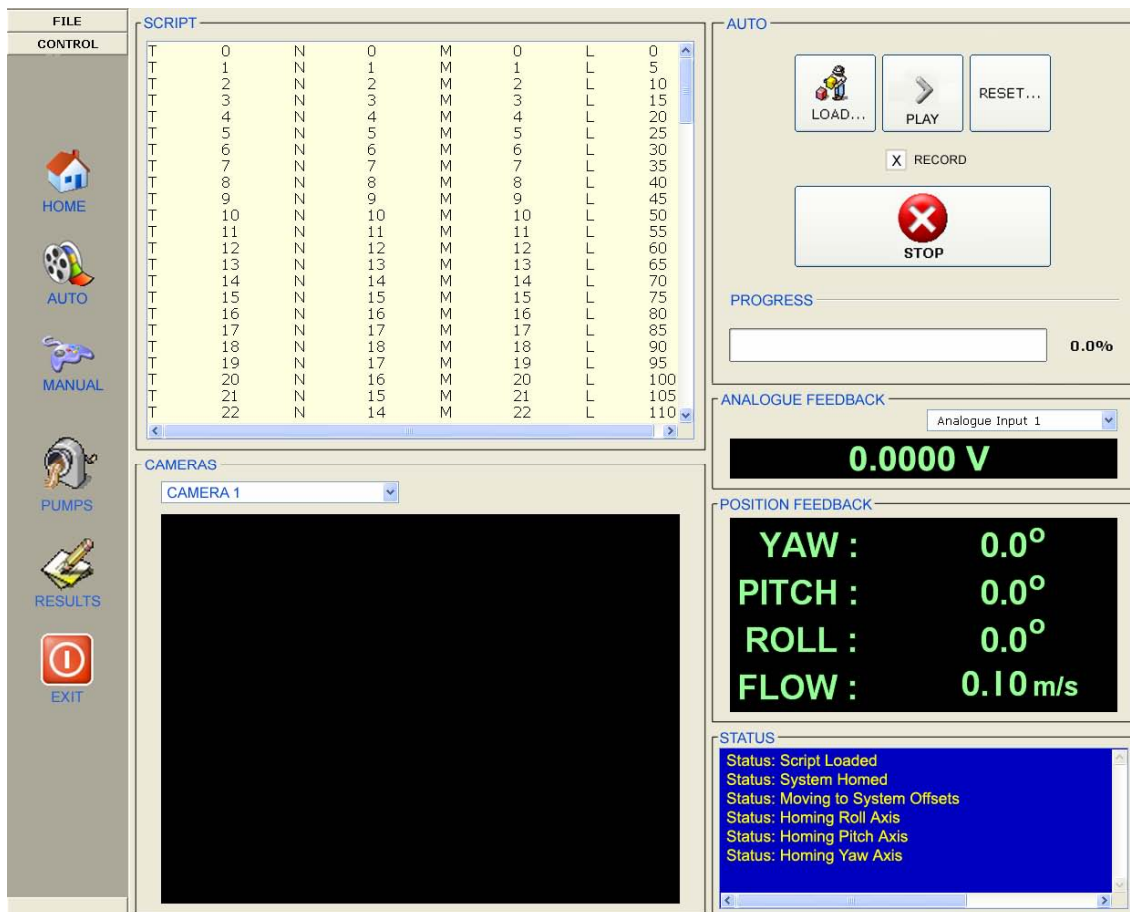


Figure 11. Graphical user interface, showing the AUTO window.

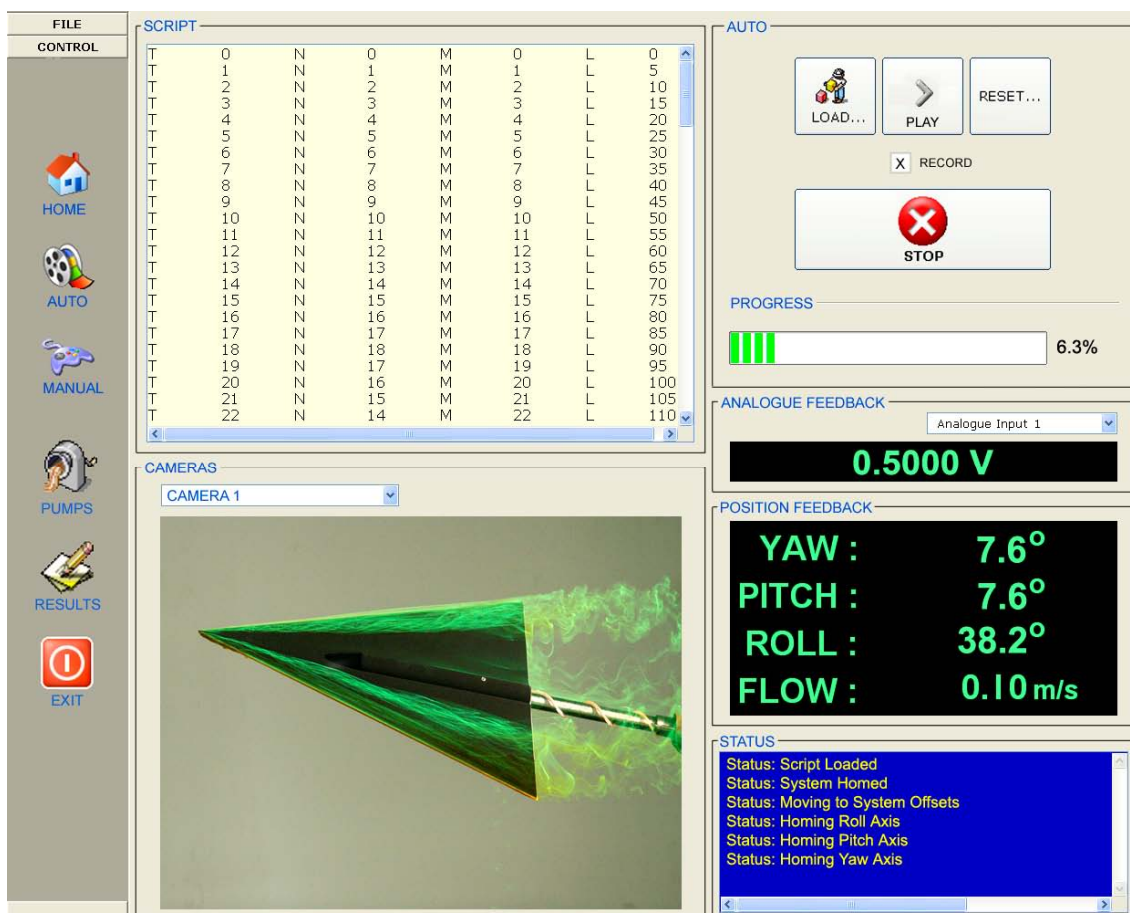


Figure 12. Graphical user interface, showing the AUTO window.

7.6.3 Writing of Data to Files

Throughout the chosen manoeuvre, instantaneous roll, pitch and yaw angles corresponding to time intervals of 0.04 s are written to a file. Using the data-acquisition system described in Section 7.1, output voltages from the signal-conditioning system are sampled for the same instants of time and the voltages are written to the file. The voltages are subsequently converted to forces and moments using the balance calibration relationships. Plan-view and side-view images of the flow are also captured for the same instants of time using the two SonyTM digital video cameras, and the images are stored digitally on the hard disk of the PC (cameras sample at 25 frames/s, i.e. 0.04 s between frames). The fact that all sampled dynamic data is synchronised facilitates subsequent analysis of the manoeuvre.

When the manoeuvre has been completed, it is necessary to click on the RESULTS icon on the left-hand side of the interface and enter the name of the file for the run. Four different files are automatically created for each run, namely

- (1) a spreadsheet file, containing sampling time instants, tunnel free-stream velocities, model orientation angles, and output voltages from the signal-conditioning system,
- (2) a file containing digital images taken by camera 1,
- (3) a file containing digital images taken by camera 2 and
- (4) a project file, which is used to manage the files when examining the manoeuvre (see Section 7.8).

7.6.4 Dynamic Tare Runs

During a dynamic manoeuvre, there are contributions to the measured forces and moments from three different sources, namely

- (1) the inertial forces and moments on the model due to its motion,
- (2) the cyclical variation of the model weight and buoyancy,
- (3) the aerodynamic flow-induced forces and moments on the model due to water flowing over the model.

As already indicated in Section 3, the inertia loads are very small for dynamic manoeuvres in a low-velocity water tunnel. To isolate the desired aerodynamic loads, item (3), it is necessary to measure the forces and moments due to (1) and (2) by carrying out a dynamic tare run with the water not flowing, and then to subtract these tare loads from the combined loads measured with the water flowing. Tare runs can be done both directly before, and directly after, measuring flow-induced loads on the model, and the corrections can be obtained by linearly interpolating between the two tare runs.

7.6.5 Averaging Loads

When a model is in motion, it is only possible to take one reading of the forces and moments at each chosen instantaneous orientation of the model as it moves through the manoeuvre. To smooth out the inevitable aerodynamic unsteadiness that occurs in the

flow, it is necessary to repeat the dynamic manoeuvre several times and average the loads measured at each of the chosen instantaneous orientations. The dynamic tare runs for a given manoeuvre can also be repeated to obtain average tare loads to be used when isolating the aerodynamic loads. It is not meaningful or practical to average the images of the flow corresponding to each measurement point, so representative images of the flow at the measurement points would normally be chosen when presenting flow patterns.

7.7 Manually Setting Model Roll, Pitch and Yaw Positions

It is often convenient to manually adjust the orientation of a model, such as when carrying out static testing in the tunnel. To do this, it is first necessary to click the MANUAL icon on the interface so that the MANUAL window appears, as shown in Figure 13. Required changes to the roll, pitch or yaw angles can be specified in terms of angular rates, in deg/s, or alternatively in terms of angular steps, in deg/step. Either the RATE or STEP button on the MANUAL window has to be clicked and then the angular rates or the angular steps have to be set as required using slider bars.

The rate of change of the pitch and yaw angles can be set between 0.0 and 2.0 deg/s, in increments of 0.02 deg/s, i.e. 100 steps, and the rate of change of the roll angle can be set between 0.0 and 10.0 deg/s, in increments of 0.1 deg/s, i.e. 100 steps. The maximum rates of change of the angles in manual control is smaller than the rates obtainable during an automatic manoeuvre, to enable fine control of each motion. The step changes in the roll, pitch and yaw angles can be set between 0.0 and 10.0 deg/step, in increments of 0.1 deg/step, i.e. 100 steps.

Once the settings have been entered, the orientation angles can be increased or decreased, one at a time, by simply positioning the cursor over the appropriate arrow on the MANUAL window and (1) for the rate setting, keeping the mouse button depressed while motion takes place, or (2) for the step setting, clicking the mouse button once. The instantaneous orientation of the model during the repositioning can be read from the POSITION FEEDBACK window. Roll, pitch and yaw angles can be varied between 0° and $\pm 360^\circ$, 0° and 65° and -20° and $+20^\circ$ respectively. The model can be set to its original orientation, i.e. its orientation prior to the manual adjustment(s), by clicking on the ZERO button in the MANUAL window.

7.8 Examination of Dynamic Data

To examine sampled dynamic data, it is necessary to launch program WTDR DATA and open a chosen project file so that images of the flow and corresponding parameters are displayed on the interface, as shown in Figure 14 (for a typical instant of time). The interface shows:

- (1) a chosen instant of time,
- (2) the tunnel free-stream velocity,
- (3) the aircraft roll, pitch and yaw angles,

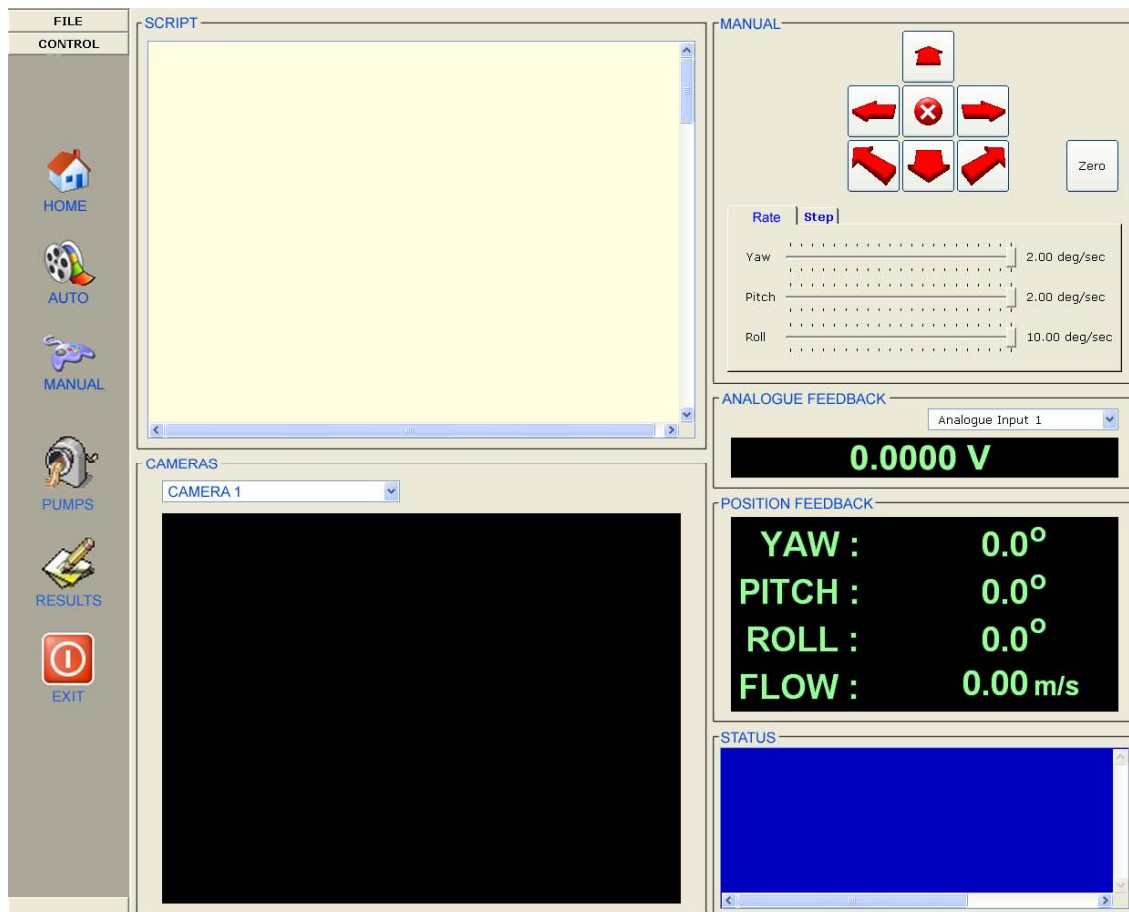


Figure 13. Graphical user interface, showing the MANUAL window.

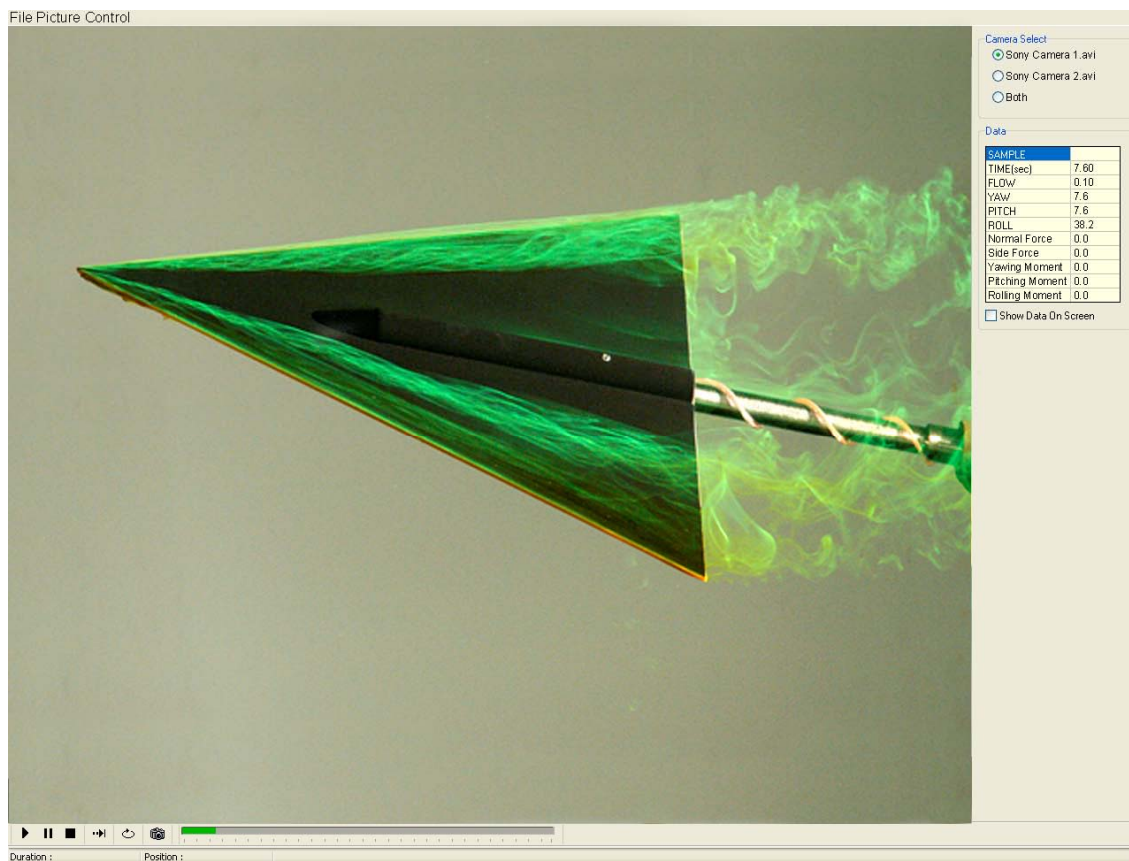


Figure 14. Graphical user interface, used when examining sampled data.

- (4) the corrected forces and moments on the aircraft (values of loads are shown as 0.0 since a balance was not used for the test manoeuvre) and
- (5) plan- and/or side-view images of the flow.

By checking the camera radio buttons, it is possible to display plan-view images only, side-view images only, or side- and plan-view images simultaneously, with a main image and a minor inset image. It is possible to play back the dynamic manoeuvre, either continuously or one step at a time, with the ability to pause at any instant of time. It is therefore possible to assess directly how loads on the aircraft are affected by different types of flow patterns over the aircraft. During playback, individual images can be saved to a file, with the corresponding values of the time instant and the roll, pitch and yaw angles imprinted on the image.

7.9 Acquisition of Static Data

It is possible to use the dynamic-testing system to acquire static data, where an aircraft is stationary at each chosen orientation when data is sampled. It is necessary to create a script file (see Section 7.4) that incorporates dwell periods, so that an aircraft can be moved through a range of orientations, such as an α sweep, in a stepwise manner. The aircraft remains stationary at a given orientation for a specified period of time before moving to the next setting, where it remains stationary again, and so on throughout a profile. As for the dynamic case, it is necessary to carry out static tare runs to enable aerodynamic flow-induced loads to be determined.

8. Tests Using a Delta Wing

Commissioning tests were carried out on a 70° delta wing to check the accuracy of the results from the new rig when compared with data given in the literature. A delta wing is an ideal test model to use when comparing data obtained in different wind and water tunnels. The reason for this is that the flow over such a wing in different facilities is consistent and well defined, and the way the associated normal forces and pitching moments vary with angle of attack are well established.

8.1 Details of Delta Wing

The delta wing used in the experiments is shown in Figure 15. The wing is made from clear Perspex. The leading edges of the wing are square to the leeward (suction) surface for the first 0.5 mm from that surface, and they are then bevelled at an angle of 30° as shown. The mean aerodynamic chord (\bar{c}) is $2/3$ of the root chord, i.e. $\bar{c} = (2/3) C_0 = 200.0$ mm. The coordinate system (x, y, z) is as shown. A metal tubular insert is embedded in the wing along its centreline to allow the model to be fitted onto a strain-gauge balance, and the insert is faired into the windward and leeward sides of the wing as shown. The two-component strain-gauge balance was positioned in the insert so that the origin of the balance coordinate system was located at the 50% \bar{c} position shown in Figure 15.

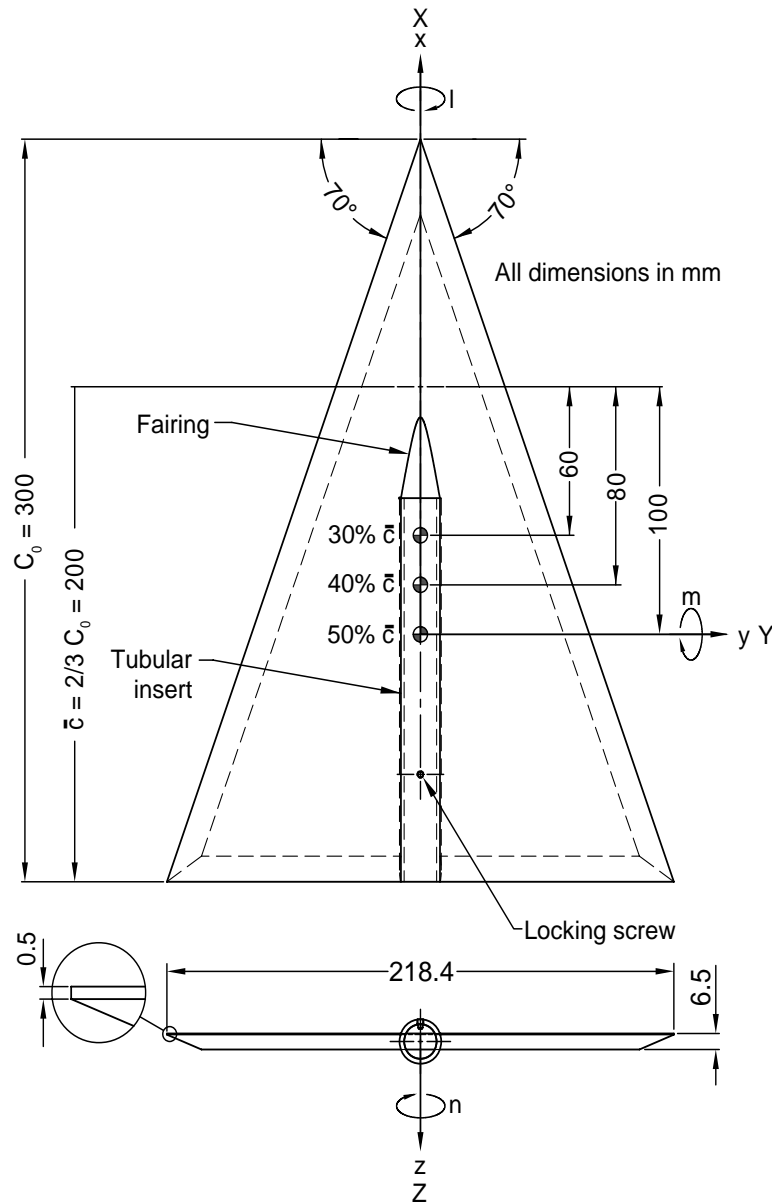


Figure 15. Delta wing used in the DSTO experiments

8.2 Static Pitching Tests

Erm (2006) measured normal forces and pitching moments on the delta wing for static values of α varying from 0° to 60° , in increments of 2° . The data were taken in the DSTO water tunnel for a free-stream velocity of 0.1 m/s. Normal-force coefficients, C_N , corrected for blockage, are shown in Figure 16, and corresponding pitching-moment coefficients, C_m , referenced to the 30%, 40% and 50% \bar{c} positions, which are located 60, 80 and 100 mm respectively from the leading edge of the mac, are shown in Figure 17. For the Erm (2006) data shown in Figures 16 and 17, each experimental point corresponds to 50 sets of gauge output voltages sampled at 1 s intervals per set.

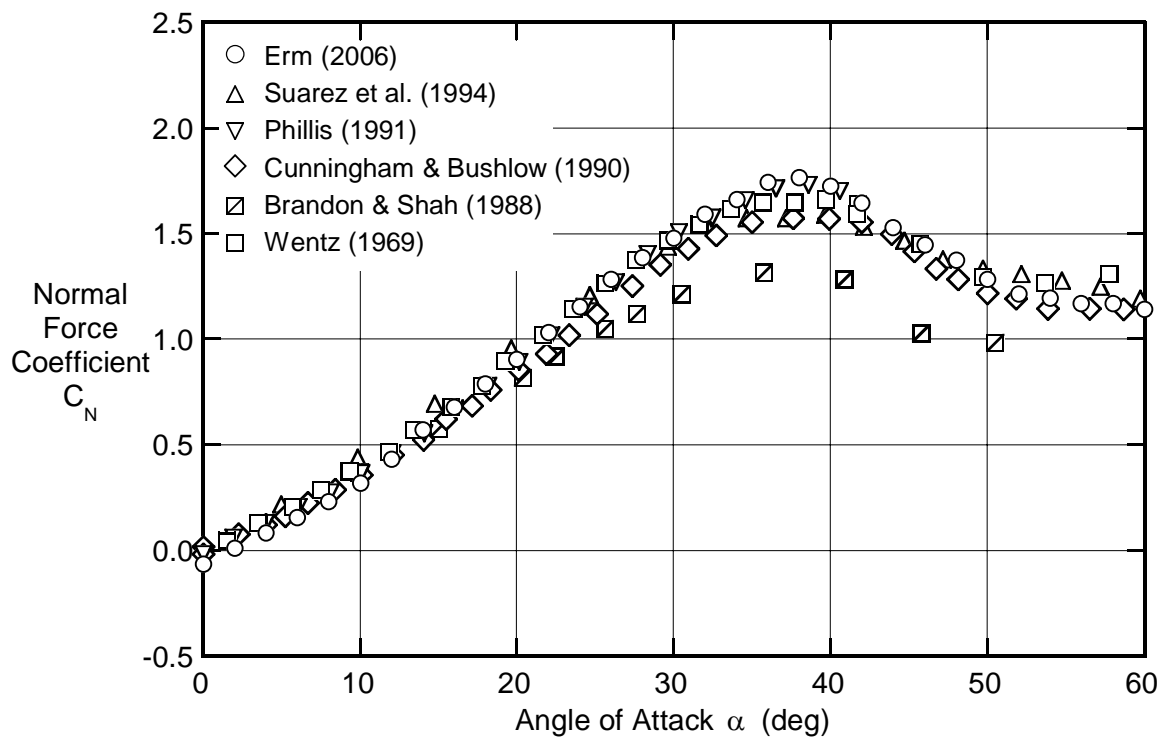


Figure 16. Normal-force coefficients for the DSTO delta wing, measured with the wing stationary at each value of α , compared with data obtained by other researchers.

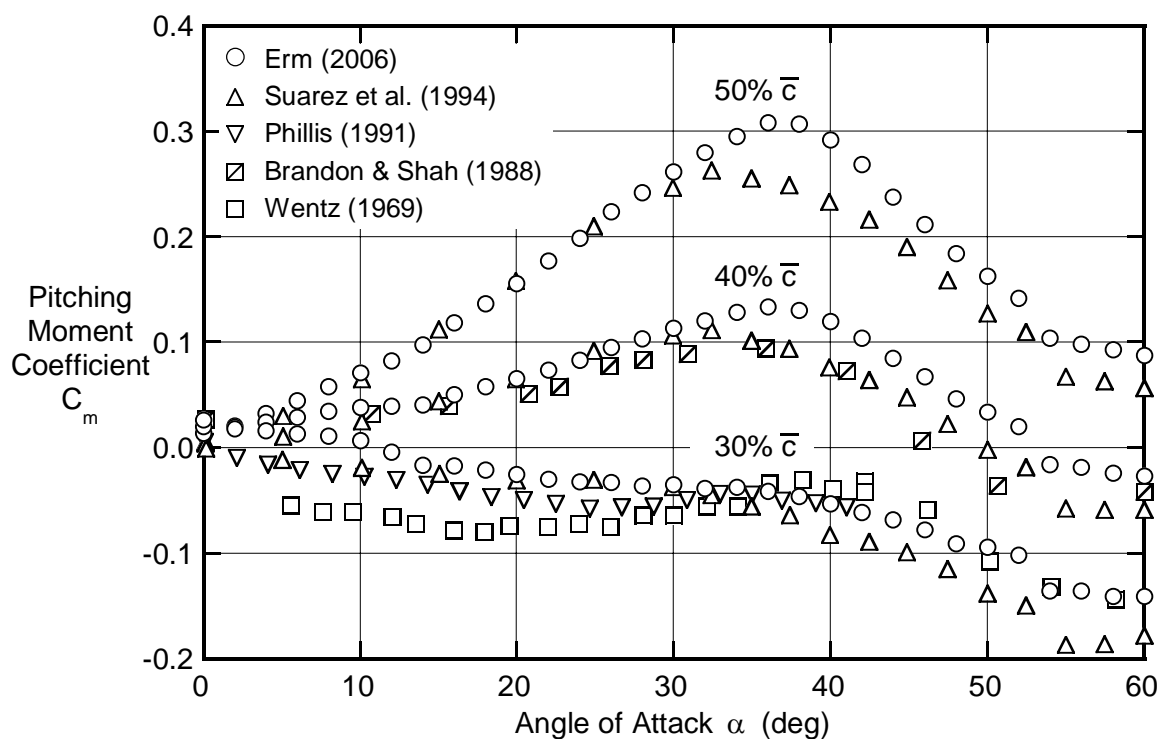


Figure 17. Pitching-moment coefficients for the DSTO delta wing, measured with the wing stationary at each value of α , compared with data obtained by other researchers.

For comparison purposes, C_N and C_m data taken on 70° delta wings in other tunnels are also plotted on Figures 16 and 17 respectively. Data of Suárez *et al.* (1994) (water tunnel), Phillis (1991) (wind tunnel), Cunningham & Bushlow (1990) (water tunnel), Brandon & Shah (1988) (wind tunnel) and Wentz (1969) (wind tunnel) are shown. There is good agreement between the DSTO data and that given by other researchers. Variation between the different sets of data could be due to differences in Reynolds numbers, flow quality, flow blockage, and the fact that the leading edges of the wings were not always the same. For example, the leading edges of the DSTO delta wing were only bevelled on one side (see Figure 15), whereas the leading edges of the delta wing used by Suárez *et al.* (1994) were bevelled on both sides.

8.3 Dynamic Pitching Tests

8.3.1 Force/Moment Measurements

Normal forces and pitching moments were measured on the DSTO delta wing when the wing was undergoing oscillatory pitching motions. To enable the dynamic data to be compared with the water-tunnel data of Suárez *et al.* (1994), the sinusoidal pitching motions used for the current tests were chosen to be dynamically similar. For Suárez *et al.*, the reduced frequency of oscillation for the pitching motion, $k = \pi f \bar{c} / U$, had a value of 0.0376 ($\bar{c} = 0.254$ m). For this value of k , their wing was oscillated with angular simple harmonic motion about four different mean angles of attack, viz. $\alpha_0 = 22^\circ, 27^\circ, 32^\circ$ and 37° , varying by $\pm 18^\circ$ from each of the four different values of α_0 . For the DSTO tests, k was 0.0376, \bar{c} was 0.200 m and U was 0.1 m/s, so that f was calculated to be 0.00598 Hz, corresponding to a time of 167.1 s for a full cycle. The instantaneous value of α throughout a dynamic manoeuvre is given by $\alpha = \alpha_0 + \Delta\alpha$, where $\Delta\alpha = 18\sin(2\pi ft)$ and t denotes the time from the start of the manoeuvre.

DSTO dynamic C_N data is compared with that of Suárez *et al.* (1994) in Figure 18 and corresponding C_m data for the 50% \bar{c} reference position is compared in Figure 19. Note that although DSTO data was acquired from $t = 0$ to 250.7 s (almost one and a half complete sine-wave cycles), only data taken over the time interval $t = 41.8$ to 208.9 s, corresponding to one complete cycle, are given in this report. Data taken prior $t = 41.8$ s (corresponding to $\Delta\alpha = 0^\circ$ to $+18^\circ$) are not given, since wing motion starts from rest at $t = 0$ s, and the flow over the wing near the start of the motion may be different from the flow over the wing when the motion is well established. The DSTO dynamic data given in Figures 18 and 19 is the average of 3 dynamic runs.

The DSTO dynamic measurements and those obtained by Suárez *et al.* (1994) have approximately the same magnitudes and show similar trends. The reasons for the relatively small differences between the two sets of dynamic data could be the same as those given in Section 8.2 for the static data.

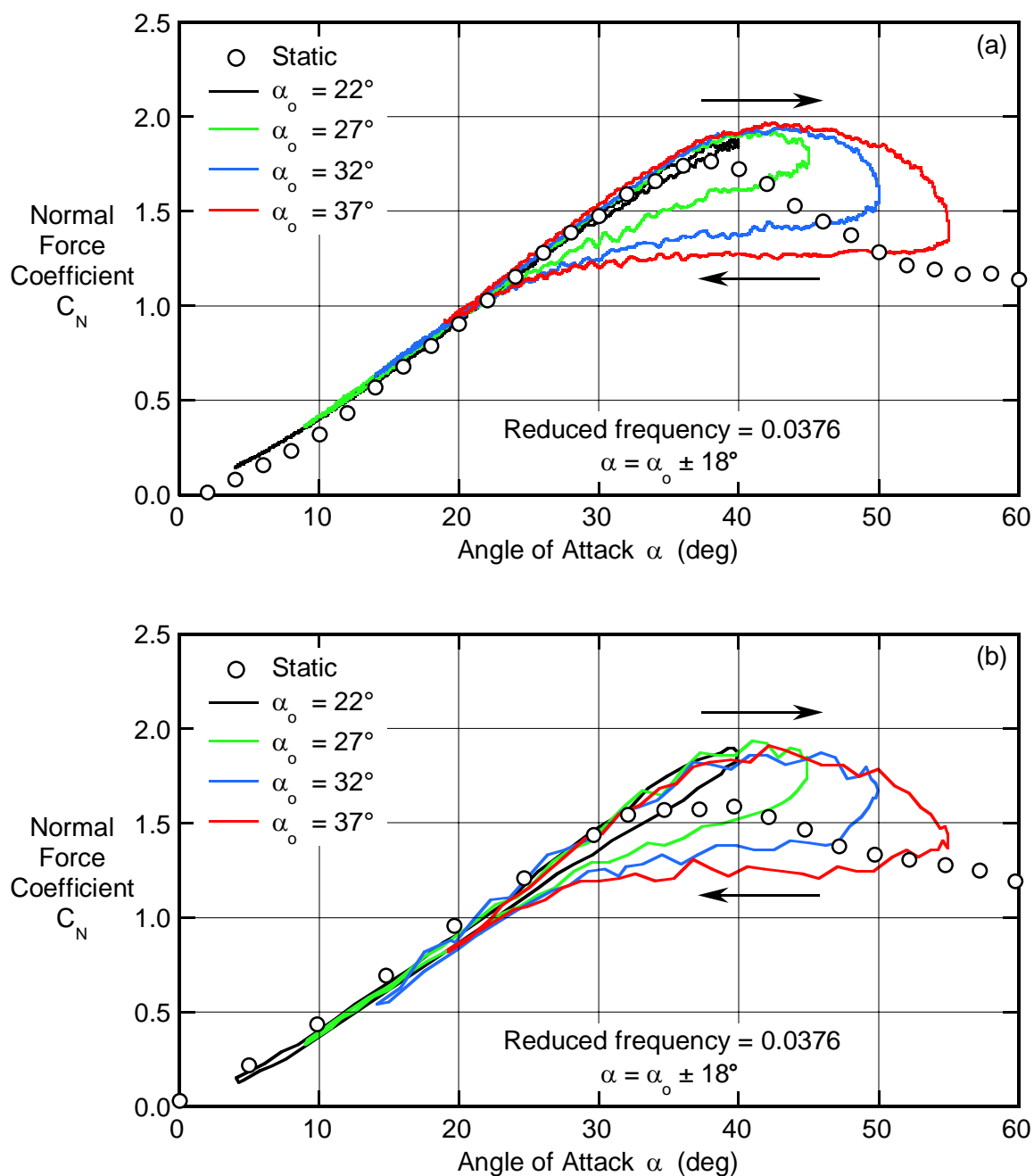


Figure 18. Normal-force coefficients for the DSTO delta wing, measured with the wing in motion, compared with corresponding data obtained by Suárez et al. (1994).
(a) DSTO data, (b) data of Suárez et al.

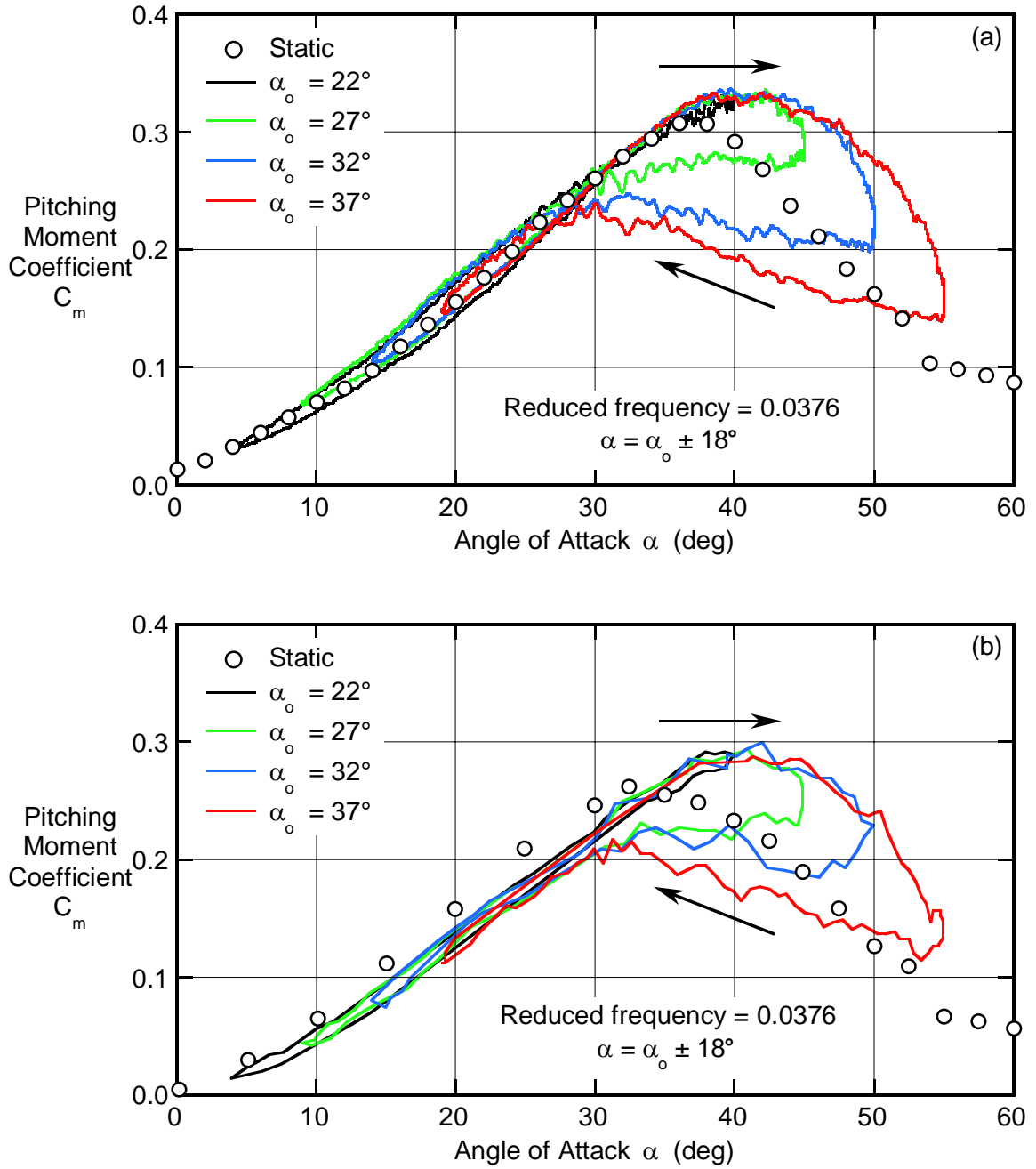


Figure 19. Pitching-moment coefficients for the DSTO delta wing, measured with the wing in motion, compared with corresponding data obtained by Suárez et al. (1994). (a) DSTO data, (b) data of Suárez et al.

8.3.2 Images of the Flow

The flow over a delta wing at an angle of attack has been studied extensively by researchers. The flow is dominated by two large bound counter-rotating vortices that are formed by the rolling up of the flow that separates along the two leading edges of the wing. These vortices produce intense suction peaks on the wing surface under their cores and this contributes significantly to the lift on the wing. As α increases, the pressure on the leeward side of the wing decreases and the cores of the vortices can become unstable and they break down or burst. The breakdown is characterised by a sudden expansion in the size of the vortex core, a rapid deceleration of the axial velocity in the core, a steep increase in the pressure and an increase in the turbulence downstream of the breakdown region. As α increases, the breakdown region moves towards the apex of the wing.

During the foregoing dynamic tests on the delta wing, the vortical flow was visualized using sodium fluorescein dye to gain an insight into how the flow was affected by the motion. Figure 20 shows images of the flow when the wing was undergoing sinusoidal pitching motion about $\alpha_0 = 32^\circ$, varying by $\pm 18^\circ$ from α_0 , with a reduced frequency of oscillation of 0.0376, as well as an image of the flow when the wing was stationary. Each image in Figure 20 corresponds to $\alpha = 32^\circ$, but α is increasing in Figure 20a, α is fixed in Figure 20b and α is decreasing in Figure 20c. The location of vortex breakdown for increasing α can be seen to lag that for the corresponding static case, and likewise for decreasing α . In other words, for increasing α , the breakdown occurs at a location further away from the apex than for the static case at the same α , and conversely for decreasing α . For increasing α , the motion of the wing into the body of water on the leeward side of the wing tends to push the vortices towards the surface of the wing, which increases the lift on the wing, and conversely for decreasing α . During oscillatory pitching motion, the lag in the movement of the breakdown region and the movement of the vortices towards or away from the wing surface affects the aerodynamic forces and moments on the wing, which in turn causes the hysteresis loops shown in Figures 18 and 19.

8.4 Coning Tests

Coning tests were carried out using the delta wing to demonstrate some of the capabilities of the dynamic-testing system. Figure 21 shows the vortical flow pattern over the delta wing during coning motion when the wing was set at a pitch angle of 32° . The non-dimensional coning rate of the wing, Ω , had a value of 0.150, and the coning rate was 0.137 rad/s (7.87 deg/s), corresponding to a time of 45.7 s for a full cycle. The wing rotated in a clockwise direction when viewed looking upstream. The tests were done for a free-stream velocity of 0.1 m/s. The coning motion causes the starboard vortex to move towards the apex of the wing and the port vortex to move away from the apex, compared with their locations for the static case (see Figure 20b). There is a slight skewing of the vortices towards port as a result of the coning motion.

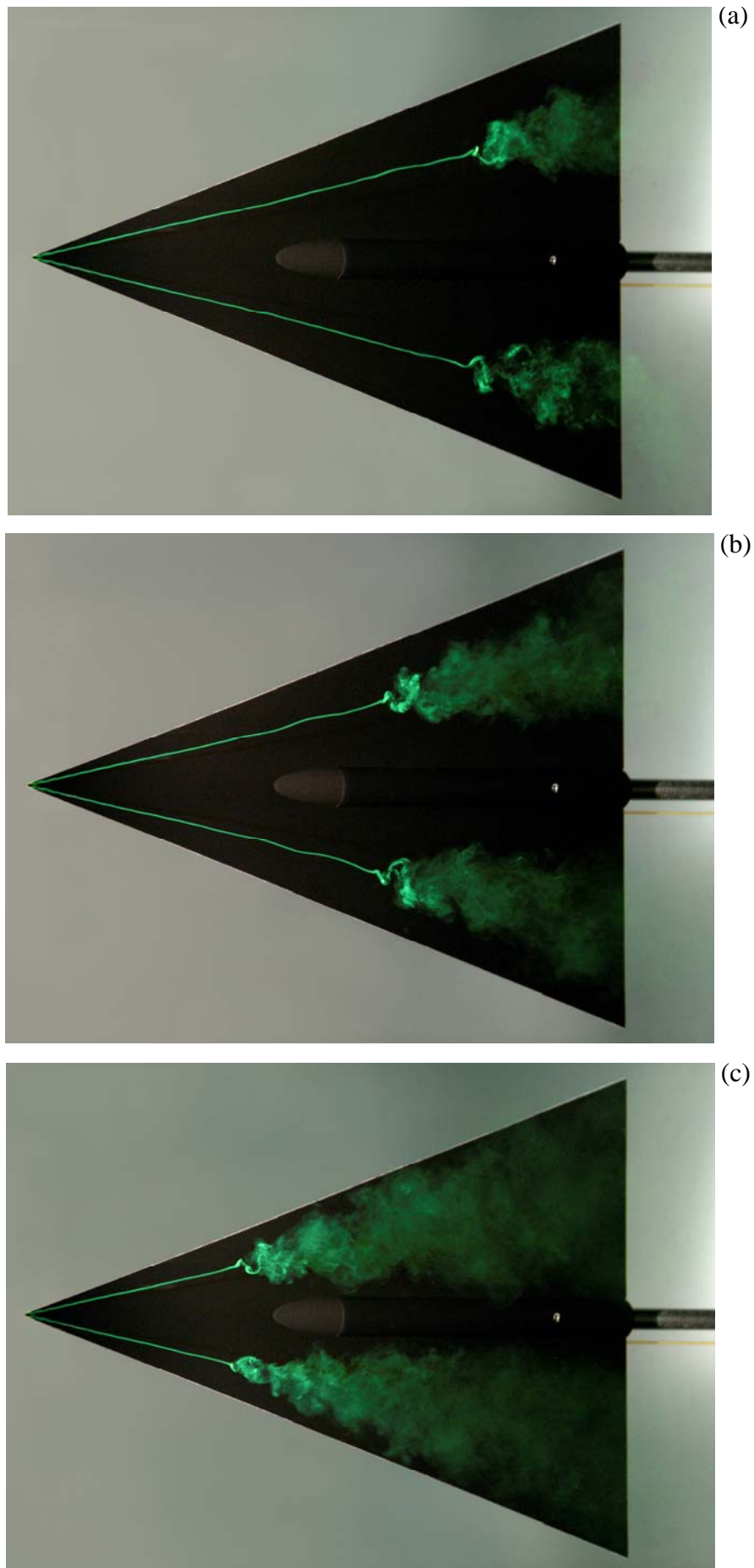


Figure 20. Flow over a delta wing, pitching tests.
(a) $\alpha = 32^\circ$, increasing α , (b) $\alpha = 32^\circ$, static, (c) $\alpha = 32^\circ$, decreasing α .

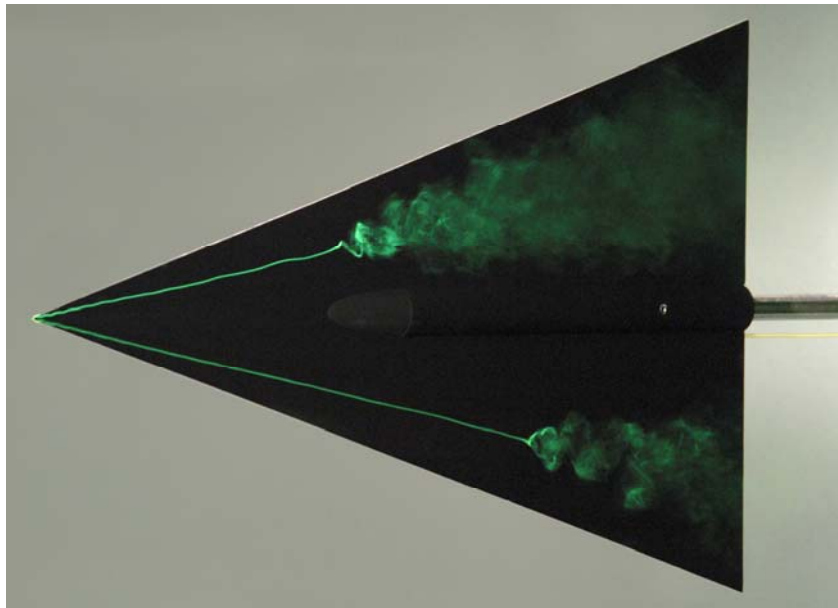


Figure 21. Flow over a delta wing, coning tests, pitch angle = 32° , clockwise rotation when viewed looking upstream.

9. Concluding Remarks

This report gives details of the development and use of a water-tunnel dynamic-testing system, where loads on a model can now be measured and corresponding images of the flow over the model captured while the model is in motion. Previously, all loads were measured and images were captured using a stationary model. A reason for developing the testing system for a water tunnel, rather than a wind tunnel, is that required rotation rates in a water tunnel to simulate a scaled dynamic manoeuvre are over 100 times slower than those for a wind tunnel, which simplifies testing procedures.

The model support system on the tunnel has been upgraded so that accurately controlled roll, pitch and yaw motions of an aircraft can now be simulated, whereas previously it was only possible to impart approximate pitch and yaw motions. For the upgraded system, roll, pitch and yaw angles can be varied between 0° and $\pm 360^\circ$, 0° and 65° and -20° and $+20^\circ$ respectively. The maximum obtainable roll, pitch and yaw rotational speeds are 12, 6 and 8 deg/s respectively. A coning mechanism has also been built where the pitch angle can be set between 0° and 35° . A sensitive two-component strain-gauge balance has been built and used to measure normal forces and pitching moments. Details of the balance are given by Erm (2006). The operation of the system, including data acquisition, is controlled via a PC using dedicated software.

Data acquisition has been synchronized so that forces and moments on a model are measured, images of the flow are captured, and the roll, pitch and yaw angles of the model are recorded, for the same instants of time throughout a dynamic manoeuvre.

Thus, the way in which changing flow conditions over an aircraft affect forces and moments on the aircraft throughout the manoeuvre can be analysed and interpreted.

The new dynamic-testing system has some unique features compared with water-tunnel dynamic-testing systems developed elsewhere. A special roll mechanism has been built so that dye can be discharged from ports on an aircraft and water can be sucked through its intake(s), to simulate engine-intake flow, while the aircraft undergoes continuous roll, i.e. there is no twisting of dye or suction tubes. It is possible to measure flow-induced loads on an aircraft during a dynamic manoeuvre, including a coning manoeuvre, while simulating engine intake flow.

The new facility was used to measure static and dynamic normal forces and pitching moments on a 70° delta wing for different angles of attack. Measured normal-force and pitching-moment coefficients agreed well with published wind- and water-tunnel data, showing that the facility gives credible results, at least for a sharp-edged delta wing, where flow patterns are independent of Reynolds number. Dynamic testing programs using aircraft will be reported at a later date.

It will now be possible to study the unsteady and highly non-linear flow associated with extreme manoeuvring and to obtain an understanding of the physics of the flow processes involved. Acquired dynamic load data can be used in flight-dynamic models, and to help validate CFD models.

10. Acknowledgements

The author is grateful for the help given by the following people. The project was substantial and could not have been completed without their significant input.

- | | |
|---------------------------------|---|
| Owen Holland | • For work done on the model-motion system, in particular liaising with Motion Solutions Australia Pty Ltd. |
| Michael Konak | • For recommissioning an existing strain-gauge-balance signal-conditioning system and for writing software for a data-acquisition system. |
| Phil Ferrarotto | • For mounting the semi-conductor strain gauges onto the chassis of the balance and for waterproofing the balance. |
| Justin Young | • For additions to the software for the dynamic-testing system. |
| Chris Jones
Ken Morgan | • For work done on the detailed design and manufacture of rig components. |
| Dennis Carnell
Kevin Desmond | • For help acquiring experimental data. |

11. References

- Brandon, J. M. & Shah, G. H. 1988 Effect of large amplitude pitching moments on the unsteady aerodynamic characteristics of flat-plate wings. Paper 88-4331-CP, *AIAA Atmospheric Flight Mechanics Conference*, Minneapolis, MN, USA, Aug 15-17.
- Brandon, J. M. & Shah, G. H. 1990 Unsteady aerodynamic characteristics of a fighter model undergoing large-amplitude pitching motions at high angles of attack. Paper 90-0309, *AIAA 28th Aerospace Sciences Meeting*, Reno, NV, USA, Jan 8-11.
- Cai, H. J. & Beyers, M. E. 2002 Overview of rotary flow visualization results on the F/A-18 aircraft. *23rd International Congress of Aeronautical Sciences*, Toronto, Canada.
- Cunningham, A. M. Jr. & Bushlow, T. 1990 Steady and unsteady force testing of fighter aircraft models in a water tunnel. Paper 90-2815-CP, *AIAA 8th Applied Aerodynamics Conference*, Portland, OR, USA, Aug 20-22.
- Ericsson, L. E. & Beyers, M. E. 1998 Wind-tunnel aerodynamics in rotary tests of combat aircraft models. *Journal of Aircraft*, Vol. 35, No. 4, Jul-Aug.
- Erm, L. P. 2006 Development of a Two-Component Strain-Gauge-Balance Load-Measurement System for the DSTO Water Tunnel. *DSTO-TR-1835*, Defence Science and Technology Organisation, Melbourne, Australia.
- Huang, X. Z. & Hanff, E. S. 2001 Motion effects on leading-edge vortex behaviour over delta wings and generalized modelling. *Symposium on Vortex Flow and High Angle of Attack Aerodynamics*, Loen, Norway, May 7-11.
- Kramer, B. R., Suárez, C. J., Malcolm, G. N. & Ayers, B. F. 1994 F/A-18 Forebody Vortex Control, Volume 2 –Rotary-Balance Tests. *NASA Contractor Report 4582*.
- Orlik-Rückemann, K. J. & Chambers, J. R. 1990 Introduction. *AGARD Advisory Report No. 265*, Report of the Fluid Dynamics Panel, Working Group 11, Rotary-Balance Testing for Aircraft Dynamics.
- Phillis, D. L. 1991 Force and pressure measurements over a 70° delta wing at high angles of attack and sideslip. Masters Thesis, Aeronautical Engineering Department, The Wichita State University, USA.
- Suárez, C. J. & Malcolm, G. N. 1995 Dynamic water tunnel tests for flow visualization and force/moment measurements on maneuvering aircraft. Paper 95-1843-CP, *AIAA 13th Applied Aerodynamics Conference*, San Diego, CA, USA, Jun 19-22.
- Suárez, C. J., Malcolm, G. N., Kramer, B. R., Smith, B. C. & Ayers, B. F. 1994 Development of a multicomponent force and moment balance for water tunnel applications, Volumes I and II. *NASA Contractor Report 4642*.
- Wentz, W. H. Jr. 1969 Wind tunnel investigations of vortex breakdown on slender sharp-edged wings. PhD Dissertation, University of Kansas, Lawrence, KS, USA.

DISTRIBUTION LIST

Development and Use of a Dynamic-Testing Capability for the DSTO Water Tunnel

Lincoln P. Erm

AUSTRALIA

Defence Organisation S&T Program	No. of Copies
Chief Defence Scientist	1
Deputy Chief Defence Scientist Policy	1
AS Science Corporate Management	1
Director General Science Policy Development	1
Counsellor Defence Science, London	Doc Data Sheet
Counsellor Defence Science, Washington	Doc Data Sheet
Scientific Adviser to MRDC, Thailand	Doc Data Sheet
Scientific Adviser Joint	1
Navy Scientific Adviser	Doc Data Sheet & Dist List
Scientific Adviser – Army	Doc Data Sheet & Dist List
Air Force Scientific Adviser	1
Scientific Adviser to the DMO	1
Deputy Chief Defence Scientist Platform and Human Systems	Doc Data Sht & Exec Summary
Chief of Air Vehicles Division: D. Wyllie	Doc Data Sht & Dist List
Research Leader Flight Systems: D. Graham	1 Printed
Head Flight Mechanics: J. Drobik	1 Printed
Head Experimental Aerodynamics, Vibration and Aeroelasticity: N. Matheson	1 Printed
Head Air Vehicle Systems Analysis: S. Henbest	1 Printed
L. Erm	9 Printed
V. Baskaran	20 Printed
M. Giacobello	
O. Levinski	
A. Blandford	P. Manovski
G. Brian	D. Newman
J. Clayton	P. O'Connor
K. Desmond	D. Sherman
P. Ferrarotto	B. Woodyatt
R. Geddes	S. Lam
DSTO Library and Archives	
Library Fishermans Bend	Doc Data Sheet
Library Edinburgh	1 printed
Defence Archives	1 printed

Capability Development Executive

Director General Maritime Development	Doc Data Sheet
Director General Capability and Plans	Doc Data Sheet
Assistant Secretary Investment Analysis	Doc Data Sheet
Director Capability Plans and Programming	Doc Data Sheet

Chief Information Officer Group

Head Information Capability Management Division	Doc Data Sheet
Director General Australian Defence Simulation Office	Doc Data Sheet
AS Information Strategy and Futures	Doc Data Sheet
Director General Information Services	Doc Data Sheet

Strategy Executive

Assistant Secretary Strategic Planning	Doc Data Sheet
Assistant Secretary International and Domestic Security Policy	Doc Data Sheet

Navy

Maritime Operational Analysis Centre, Building 89/90 Garden Island Sydney NSW	Doc Data Sht & Dist List
Deputy Director (Operations)	
Deputy Director (Analysis)	
Director General Navy Capability, Performance and Plans, Navy Headquarters	Doc Data Sheet
Director General Navy Strategic Policy and Futures, Navy Headquarters	Doc Data Sheet

Air Force

SO (Science) - Headquarters Air Combat Group, RAAF Base, Williamstown NSW 2314	Doc Data Sht & Exec Summary
Staff Officer Science Surveillance and Response Group	Doc Data Sht & Exec Summary

Army

ABCA National Standardisation Officer

Land Warfare Development Sector, Puckapunyal	Doc Data Sheet
J86 (TCS GROUP), DJFHQ	Doc Data Sheet
SO (Science) - Land Headquarters (LHQ), Victoria Barracks NSW	Doc Data Sht & Exec Summary
SO (Science) - Special Operations Command (SOCOMD), R5-SB-15, Russell Offices Canberra	Doc Data Sht & Exec Summary
SO (Science), Deployable Joint Force Headquarters (DJFHQ) (L), Enoggera QLD	Doc Data Sheet

Joint Operations Command

Director General Joint Operations	Doc Data Sheet
Chief of Staff Headquarters Joint Operations Command	Doc Data Sheet
Commandant ADF Warfare Centre	Doc Data Sheet
Director General Strategic Logistics	Doc Data Sheet

Intelligence and Security Group

AS Concepts, Capability and Resources	1
DGSTA , Defence Intelligence Organisation	1

Manager, Information Centre, Defence Intelligence Organisation	1
Director Advanced Capabilities	Doc Data Sheet

Defence Materiel Organisation

Deputy CEO	Doc Data Sheet
Head Aerospace Systems Division	Doc Data Sheet
Head Maritime Systems Division	Doc Data Sheet
Program Manager Air Warfare Destroyer	Doc Data Sheet
Guided Weapon & Explosive Ordnance Branch (GWEO)	Doc Data Sheet
CDR Joint Logistics Command	Doc Data Sheet

OTHER ORGANISATIONS

National Library of Australia	1
NASA (Canberra)	1

UNIVERSITIES AND COLLEGES

Australian Defence Force Academy

Library	1
Head of Aerospace and Mechanical Engineering	1

Monash University:

Hargrave Library,	Doc Data Sheet
Professor J. Soria,	1 Printed

University of Adelaide: Professor R. M. Kelso	1 Printed
--	-----------

University of Melbourne:

Engineering Library	1 Printed
Emeritus Professor P. N. Joubert	1 Printed
Professor M. S. Chong	1 Printed

OUTSIDE AUSTRALIA

ORGANISATIONS

Air force Research Laboratory	
Dr. M. Ol	1 Printed
Rolling Hills Research Corporation:	
Dr B. R. Kramer	1 Printed
Dr M. F. Kerho	1 Printed

UNIVERSITIES AND COLLEGES

Princeton University: Professor A. J. Smits	1 Printed
--	-----------

University of Minnesota: Professor I. Marusic	1 Printed
--	-----------

INTERNATIONAL DEFENCE INFORMATION CENTRES

US Defense Technical Information Center	1
UK Dstl Knowledge Services	1
Canada Defence Research Directorate R&D Knowledge & Information Management (DRDKIM)	1
NZ Defence Information Centre	1

ABSTRACTING AND INFORMATION ORGANISATIONS

Library, Chemical Abstracts Reference Service	1
Engineering Societies Library, US	1

Materials Information, Cambridge Scientific Abstracts, US	1
Documents Librarian, The Center for Research Libraries, US	1

INFORMATION EXCHANGE AGREEMENT PARTNERS

National Aerospace Laboratory, Japan	1
National Aerospace Laboratory, Netherlands	1

SPARES	4 Printed
--------	-----------

Total number of copies: 74 Printed: 49 PDF: 25

DEFENCE SCIENCE AND TECHNOLOGY ORGANISATION DOCUMENT CONTROL DATA					
				1. PRIVACY MARKING/CAVEAT (OF DOCUMENT)	
2. TITLE Development and Use of a Dynamic-Testing Capability for the DSTO Water Tunnel			3. SECURITY CLASSIFICATION (FOR UNCLASSIFIED REPORTS THAT ARE LIMITED RELEASE USE (L) NEXT TO DOCUMENT CLASSIFICATION) <div style="display: flex; justify-content: space-between;"> Document (U) </div> <div style="display: flex; justify-content: space-between;"> Title (U) </div> <div style="display: flex; justify-content: space-between;"> Abstract (U) </div>		
4. AUTHOR(S) Lincoln P. Erm			5. CORPORATE AUTHOR Defence Science and Technology Organisation 506 Lorimer St Fishermans Bend Victoria 3207 Australia		
6a. DSTO NUMBER DSTO-TR-1836		6b. AR NUMBER AR-013-599		7. DOCUMENT DATE March 2006	
8. FILE NUMBER 2005/1052347/1		9. TASK NUMBER 04/182		10. TASK SPONSOR DSTO	
				11. NO. OF PAGES 31	
				12. NO. OF REFERENCES 13	
13. URL on the World Wide Web http://www.dsto.defence.gov.au/corporate/reports/DSTO-TR-1836.pdf				14. RELEASE AUTHORITY Chief, Air Vehicles Division	
15. SECONDARY RELEASE STATEMENT OF THIS DOCUMENT <p style="text-align: center;"><i>Approved for public release</i></p>					
OVERSEAS ENQUIRIES OUTSIDE STATED LIMITATIONS SHOULD BE REFERRED THROUGH DOCUMENT EXCHANGE, PO BOX 1500, EDINBURGH, SA 5111					
16. DELIBERATE ANNOUNCEMENT No Limitations					
17. CITATION IN OTHER DOCUMENTS Yes					
18. DEFTEST DESCRIPTORS Water tunnel tests, Dynamic tests, Load tests, Aircraft models					
<p>This report gives details of the development and use of a water-tunnel dynamic-testing system, whereby models of aircraft are tested as they undergo a dynamic manoeuvre, with the roll, pitch and yaw angles changing in a specified way. Traditionally, most testing of aircraft in tunnels has been done with the aircraft stationary and set at a known orientation, but the acquired static data has limited applicability to manoeuvring aircraft. Dynamic data is needed to study unsteady aerodynamic effects associated with aircraft motion, to obtain data for use in flight-dynamic models of aircraft behaviour, and when validating CFD predictions of aircraft behaviour. Using the new testing system, flow-induced loads on an aircraft model can be measured and corresponding images of the flow over the aircraft can be captured for known instantaneous orientations of the aircraft, so that the loads can be correlated with the flow patterns. During a dynamic manoeuvre, including a coning manoeuvre, loads and images can also be acquired while simulating engine-intake flows. Loads were measured on a delta wing in the water tunnel when the wing was stationary and when it was in motion. The measured loads showed good agreement with wind- and water-tunnel data reported in the literature, showing that the new testing system gives credible results.</p>					